Extrasolar Planet Transit Photometry at Wallace Astrophysical Observatory

by

Wen-fai Fong

Submitted to the Department of Physics

in partial fulfillment of the requirements for the degree of

Bachelor of Science in Physics

at the

MASSACHUSETTS INSTITUTE OF TECHNOLOGY
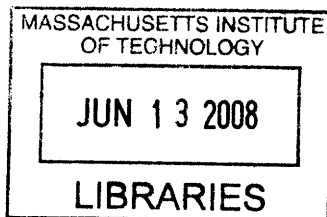
June 2008

Written by_____

σ

Department of Physics
May 9, 2008

Certified by_____

Richard P. Binzel
Thesis Supervisor, Department of EAPS

Accepted by _____

Professor David E. Pritchard
Senior Thesis Coordinator, Department of Physics

1

Extrasolar Planet Transit Photometry at Wallace Astrophysical Observatory

by

Wen-fai Fong

Abstract

Extrasolar planet transit photometry is a relatively new astronomical technique developed over the past decade. Transit photometry is the measurement of a star's brightness as an orbiting planet passes in front of the star as seen from the Earth. Recently, members of MIT's Planetary Astronomy Lab (PAL) have launched an observing program for extrasolar planet transits at Wallace Astrophysical Observatory (WAO), which houses the 24-inch telescope used in this work. The purpose of this thesis is to enable students and faculty to easily perform transit photometry at WAO and assess the feasibility of transit photometry there. The PAL extrasolar planetary database currently has 36 planetary candidates, 23 of which are observable at WAO due to their positive declinations δ (in the Northern celestial hemisphere). The maintenance of this database is described. Prediction methods used in *Mathematica* to determine when transits will occur at WAO for a given period of time are discussed. The transits at WAO are prioritized based on frequency of transit, transit depth and celestial location of parent stars, using the prediction period of 01-20-2008 to 05-30-2008. This prediction period is compared to four others spanning 2007-2009. These results suggest that the best planetary candidates at WAO for the fall are XO-3b, WASP-1b and HAT-P-6b and for the spring are HAT-P-3b, TrES-3 and XO-3b. A typical observing plan is produced based on the planetary candidate TrES-3, including finder charts for the highest frequency transiting planets in Spring 2008. Data reduction and analysis using either the standard IDL routine *phot* or the "Make_Lightcurve.nb" *Mathematica* notebook are described. A partial transit of XO-2b taken at WAO is presented. Given WAO's recent upgrade by PAL along with the data presented here, the feasibility for successful extrasolar planet transit photometry projects at WAO is high.

Thesis Supervisors:
James L. Elliot (Professor of Physics)
Richard P. Binzel (Professor of Earth, Atmospheric & Planetary Science)

Acknowledgements

This thesis would not have been possible without the following people. First and foremost, I would like to thank Prof. James Elliot for encouraging me to take on a difficult observing project when I had little experience in observational astronomy and for challenging me to always ask questions and be assertive in the lab. I would like to thank Prof. Richard Binzel for stepping in as my second advisor and helping me with the last stages of my project. Thank you to Amanda Gulbis, who was in Hawaii on an observing run but still took the time to read my 60-page thesis and give me detailed comments. Thank you to Elisabeth Adams for her never-ending knowledge of *Mathematica* and to Matthew Lockhart for his perseverance in observing at WAO, despite the frustrations the weather and technical difficulties can often bring. Thank you to fellow undergraduate Folkers Rojas for helping me to keep a positive attitude in the lab.

I must also thank the two people who have constantly encouraged me in my academic pursuit of a career in astronomy: Prof. Eric Blackman (University of Rochester) and Prof. Julia Lee (Harvard Center for Astrophysics). Thank you for cheering me on when I was losing hope!

I could not have survived the past four years without the strength and support of my parents, my two older sisters, and my best friend. Thank you for everything that you do. Without the confidence and inspiration you have all instilled in me, none of this would have been possible.

Contents

1   Introduction

1.1   *Importance of detecting extrasolar planets*

For centuries, astronomers have been limited to our own solar system as a model for studying important processes such as solar system formation, planetary formation, surface weathering, satellite and ring formation, and the requirements for the evolution of life as we know it. They have launched missions reaching as far as Pluto, which has an average distance to the Sun of 39.53 AU, where 1 AU = the average distance from the Earth to the Sun = 1.4959787 x 10^{11} m [Hartmann, 2005]. By launching these missions and collecting data through flybys, orbiters, probes and landers, they have developed theories for how our solar system formed into what it is today. However, in recent decades, astronomers have begun the search for planets outside of our solar system, or extrasolar planets, and have very been successful. Such planets can provide additional models in studying important planetary processes, as well as confirm the theories already developed.

An extensive search began in the late 1980s and the first planet detected was HD 114762b in 1989 by Latham et al. (1989). They used the radial velocity technique which is described in Section 1.3. Today, a total of 287 candidate extrasolar planets have been detected by various techniques. This thesis concerns the particular technique of transit photometry. A total of 46 extrasolar planets have been detected in this way. The first planet to be discovered by transit photometry was HD 209458b in 1999 [Schneider, 1995-2008].

1.2   *Detection of extrasolar planets by transit photometry*

The outermost reaches of our solar system, mainly comprised of the Oort Cloud, are suspected to extend to ~1 x 10^{5} AU from our Sun. Most extrasolar planetary systems lie well outside of our solar system, placing them more than 10^{6} AU away. In addition to being very

small and relatively far away, these planets also do not generate light themselves and only reflect the light of the stars that they orbit. Therefore, they are extremely faint and are rarely seen directly. To detect them, astronomers have developed various methods to find these planets indirectly. One of the main detection methods is extrasolar planet transit photometry. Just as our Earth orbits the Sun, extrasolar planets orbit a parent star with a predictable period in accordance with the laws of Keplerian orbit, which state that for an elliptically orbiting object, the square of the period of a object's orbit equals the cube of that object's semimajor axis. It follows that an extrasolar planet will have a relatively unchanging orbital period as governed by the semimajor axis of its orbit. However, most planets discovered by transit photometry have relatively short periods (< 10 days) and have nearly zero-eccentricity, or circular, orbits.

With this relatively short period, the planet may periodically cross in front of, or transit, its star if the plane of the orbit is edge-on as viewed from the Earth. This transit can be detected using photometry, or the measurement of the magnitude of the parent star. A lightcurve can be produced from several consecutive photometric measurements as a plot of the star's brightness over time, where a transit is detectable as a short duration drop in brightness. With transit photometry, we expect to find mainly short-period planets because we have a higher probability of viewing such transits if they occur more frequently.

A typical extrasolar planet transit has five stages including the ingress and egress of the transit. These five stages and their corresponding points on the lightcurve are depicted in Figure 1. The planet begins to transit the parent star at stage 2, resulting in a prolonged dip in the star's brightness until stage 4, when the transit ends. The width of the dip depends on the orbital velocity of the planet v_p, the distance from the planet to the star, and the radius of the star R_*. The transit depth d depends on the relation between the radius of the planet R_p and R_* by

$$d = \left[\frac{R_p}{R_*}\right]^2 . \tag{1}$$

Since the radius of the star is significantly higher than the radius of the planet, the transit depth is very small, ranging from ~0.002-0.03 or ~0.2-3.0% of the star's original magnitude. At present, we cannot detect d much lower than 0.2% and do not expect much higher than 3% assuming as an example our own solar system. For example, the transit depth d of our largest planet Jupiter with $R_p = 7.14 \times 10^7$ m and $R_* = R_{SUN} = 6.95 \times 10^8$ m, turns out to be 0.0105 or 1.05% [radii taken from Hartmann, 2005]. A similar calculation for the planet with the smallest radius, Mercury, yields a d on the order of 10^{-5}. These represent the upper and lower limits of d in our solar system, so we would not expect to find extrasolar planets that are significantly out of this range. However, we have found what are called hot, inflated Jupiters, which are Jupiter-sized planets closer to their parent stars than the Jupiter-Sun distance. These large planets account for the extrasolar upper limit on d of 3.0% as opposed to the expected 1.05%.

Transit photometry is unique in that it allows us to measure the radius ratio R_p/R_* directly, and compare it to the radius ratio of planets in our solar system, where $R_* = R_{SUN}$. In the absence of limb darkening, or the darkening effect an object undergoes as it moves from the center to the edge of an image, parameters such as inclination i and the semimajor axis ratio a/R_* can easily be derived from lightcurve data [Seager & Mallén-Ornelas, 2003]. These parameters may still be dervied from the lightcurve if there is limb darkening, but Seager & Mallén-Ornelas (2003) present a simplified solution for these parameters in its absence. By following standard stellar evolution models and fixing the period P of the star, Torres et al. (2008) propose that one can easily find the mass, radius, luminosity, surface gravity and age of the star through a series of standard equations [Torres, Winn & Holman 2008].

Over the past two decades, the transit photometry detection method has proved to be informative and reliable. Once the orbital period of the planet is known, the time of the next detectable transit is very predictable. Many astronomers have made prediction programs as to when the next transit for a given planet and observing location will occur, similar to the one outlined in Section 3.1 of this paper. This method only requires differential photometry with a minimum of two in-frame comparison stars and photometric capabilities to detect the ~0.2-3.0% reduction in magnitude. Differential photometry is a method that uses comparison stars in the CCD frame of the parent star in order to calculate differential magnitudes. A minimum of two such comparison stars is needed to calibrate the parent star for atmospheric fluctuations or any intrinsic variability of the telescope. This method is described mathematically in Section 6.1. With sufficient CCD photometric capabilities, it is then easy to produce several lightcurves of one planet in a single year in order to improve orbital parameters.

Although transit photometry is very reliable, it also has a few disadvantages. First, transits of extrasolar planets can only be detected when the planet's orbital plane is edge-on as viewed from the Earth. Given a narrow angle for a correct viewing geometry, this configuration is quite improbable. Therefore only a small percentage of extrasolar planet transits can actually be detected from Earth by this method. The probability of this alignment is the ratio of the star's diameter to the radius of the planet's orbit. Using this ratio for an example, the probability of Jupiter transiting our Sun is ~0.9%, and unknown factors such as clear observing conditions or correct timing in order to view a similar extrasolar transiting system might further decrease this probability. Second, the nature of transit photometry requires that the telescope and CCD system typically be sensitive enough to reliably detect a very marginal reduction in brightness on the lightcurve. We explore in this paper some of the constraints transit photometry sets on the

sensitivity of the telescope-CCD system. Third, as mentioned above, differential photometry requires at least two comparison stars in the CCD field of view. For a given parent star, not all of the in-frame stars are of comparable magnitude making it more difficult for accurate and effective differential photometry. Therefore, there are other detection methods which are more versatile in their ability to find planetary candidates but have benefited from follow-up observations by transit photometry. Although this paper is largely concerned with the method of transit photometry, a brief introduction to other common methods is provided for reference.

1.3 *Other common detection methods*

Since known extrasolar planets are very faint, all current detection methods depend on the influence of the planet on the star. Although a planet has a very small mass M_p relative to its parent star, it still has a slight gravitational influence on the star. This can cause the star to "wobble" in a periodic back-and-forth motion as the planet orbits or changes its direction with respect to the star. Using astrometry, or the measurement of the position of an object with respect to other objects, on the star, we can detect this wobble. Astrometry thus indicates if a planet may be orbiting our star of interest. However, since these back-and-forth distances are so minute, even the largest ground-based telescopes have trouble detecting these planets by astrometry. In addition, astrometry works best for planets with long periods, for which the wobble is much greater and thus, easier to detect. NASA plans to launch the Space Interferometry Mission in order to perform astrometry with much higher precision than can be done on Earth [SIM PlanetQuest, http://planetquest.jpl.nasa.gov/SIM/sim_index.cfm]. No planets have been detected by astrometry thus far.

A more successful ground-based form of detecting this wobble is by radial velocity detection. As the planet tugs on the parent star, the star's light will undergo a Doppler shift that

we can see as a tiny wavelength shift on a spectrum. For example, if the planet tugs the star such that it wobbles toward the Earth, the detected light from the star will shift toward shorter, more blue wavelengths. In contrast, a star that is influenced to wobble slightly away from Earth will give off longer, redder wavelengths. The first discovery of an extrasolar planet orbiting a sun-like star was by Mayor & Queloz (1995) using radial velocity detection on the star 51 Pegasi to find the planet 51 Peg b. Although 51 Peg b is on the order of 1 M_J (mass of Jupiter = 1.90 x 10^{27} kg [Hartmann, 2005]), it was found to orbit its parent star at a closer distance than Mercury orbits the Sun. At the time, radial velocity precision was within 13 m s^{-1} [Mayor & Queloz, 1995]. However, today professional astronomers such as Li et al. (2008) are developing instruments such as the "Astro Comb" which should allow radial velocities to be measured with a precision of 1 cm s^{-1} and therefore allow the detection of significantly smaller planets than those already discovered. To date, 271 planets have been detected by the radial velocity technique out of a total of 287 detected candidates [Schneider, 1998-2005]. This technique, even at relatively low precision, has proved to be extremely versatile.

Other detection methods are gravitational microlensing by the planet and direct imaging, but these methods are more exclusive and less widely used. Gravitational microlensing occurs when a distant star's light passes through a nearby star before it hits the observer, such that the nearby star's gravitational field acts as a lens. If the nearby star has a planet, this can be detected by the observer as well. Udalski et al. (1994) developed the Optical Gravitational Lensing Experiment (OGLE) in an attempt to detect planets by gravitational lensing. Six candidates have been detected so far and all are in the Southern celestial hemisphere [Schneider, 1998-2005]. Direct imaging is extremely difficult since planetary candidates are so faint. Imaging only works if the candidate's mass is significantly larger than 1 M_J, if the candidate is proximal to Earth

(well within 10^6 AU), or if the candidate does not have an extremely bright parent star so it can be seen separately from the parent star. Five candidates have been detected by direct imaging thus far [Schneider, 1998-2005].

1.4   *Recent planetary discoveries by transit*

There have been over 20 extrasolar planets discovered by transit photometry in the past year and a total of 46 planets detected by transit since 1999. It follows at the present that on average, a new planet is discovered with this technique slightly less than once every two weeks. Therefore, the present is a very opportune time to observe planetary transits and improve upon those parameters released in discovery papers. The concept of planet transits is quite simple, so given adequate observing equipment, extrasolar planet transits could serve as potential student projects for college-level observational astronomy classes. In this thesis, I hope to elucidate the process of extrasolar planet transit photometry at Wallace Astrophysical Observatory (WAO) by explaining the observational limitations at WAO, providing prediction methods for when transits will occur, and providing useful planetary parameters for observing transits at WAO. I will provide data analysis methods for WAO transit data and present the first extrasolar planet transit observed with the 24-inch telescope at WAO. Lastly, I will elaborate on future work at WAO in light of the data presented and the recent upgrades. This thesis will hopefully open the door to many students who wish to do a project in transit photometry within one semester.

2   Telescope & Planetary Information

2.1   *Wallace Astrophysical Observatory (WAO)*

WAO is an MIT-owned observatory located in Westford, MA. WAO consists of six telescopes: one 24-inch telescope, one 16-inch telescope, and four smaller telescopes (three 14-inch, one 11-inch) aligned in a shed with a retractable roof. The observatory's coordinates are Lat. = **42° 36.6′ N**, Long = **71° 29.1′ W**, where 1′ or 1 minute of latitude = $1/60°$.

The work for this thesis was performed with the 24-inch telescope at WAO, but I will describe the specs of shed Telescopes 3 and 4 as well because PAL recently upgraded their CCDs and transit photometry may be more feasible for students on these smaller telescopes. Telescopes 3 and 4 are 14-inch Celestron C14 Schmidt-Cassegrain telescopes each equipped with a new SBIG STL-1001E imaging charge-couple device (CCD) camera. In general, CCDs have a higher quantum efficiency than older devices such as photographic plates. This means that a higher percentage of photoelectrons are generated for each photon incident on the CCD. On shed Tel 3, the CCD field of view is 20.5′ x 20.5′ where 1′ or 1 arcminute = $1/60°$. On shed Tel 4, the CCD field of view is 23.5′ x 23.5′. These field of view dimensions are significantly larger than they were before the CCD upgrade. The detector is a 1024 x 1024 pixel array for total of approximately one million pixels. Each pixel is 24 x 24 μm. Each telescope is mounted on a Paramount ME^{TM} equatorial mount to allow for automated pointing although they can also be manually controlled. Automation is controlled on iMac computers that run Windows XP. TheSky6^{TM} is used for pointing and calibrating the position of the telescope while CCDSoft^{TM} is used for syncing the CCD with the telescope. CCDSoft^{TM} allows the user to set exposure time, number of consecutive exposures, CCD temperature, and other necessary parameters in taking customized data. More information about how this software is run can be found at Software

Bisque's website [http://www.bisque.com]. Output data are read-only FITS files that can be easily transferred to another computer for data analysis. The visual limiting magnitude, or magnitude of the faintest object detected by the human eye aided by an instrument, can roughly be calculated by

$$V_{Limit} \approx 7.5 + 5\log(D_o),$$ (2)

where D_O is the aperture of the telescope. This is a very rough estimate because it does not include sky conditions, age of the telescope-CCD system, or filter. Using the above formula, the limiting magnitude of Tel 3 and Tel 4 are ~15. The typical cloud cover and seeing conditions in Boston will decrease this limiting magnitude.

The work for this thesis was performed with the 24-inch telescope at WAO. The 24-inch telescope is an Ealing Research Cassegraine Coudé reflector, with an image scale of 23.3 ″/mm where 1″ or 1 arcsecond = 1/60′. It is used in conjunction with the POETS (Portable Occultation, Eclipse, and Transit System) CCD. Professor Jim Elliot's Planetary Astronomy Laboratory (PAL) at MIT played a large role in developing the POETS set of instruments. The idea for POETS was developed in order to optimize high-speed observations such as transits [Souza et al., 2006; Gulbis et al., 2008]. Therefore, POETS has frame-transfer (FT) capability which means that for a consecutive number of exposures, the CCD is being exposed while the previous frame is being read out. This reduces the dead readout time to almost zero. The CCD is an Andor iXon DU-897 with 512 x 512 array of 16 μm square pixels. On the WAO 24-inch telescope, the CCD field of view is 3′ 22″ x 3′ 22″, which is significantly smaller than the upgraded shed CCDs. The POETS set of instruments is particularly useful in its transportability as the entire system can fit into two carry-on sized bags [Souza et al., 2006]. POETS is currently the main

CCD used on the 24-inch telescope at WAO. Applying equation 2 gives a limiting magnitude of ~17.

Observing at WAO is ideal in several ways for staff and students. Every observational and instrumentation aspect at WAO is well-documented. It is at a convenient location because it is only a 45-minute drive from downtown Boston, but is far enough away to avoid significant light pollution. It is maintained and upgraded by PAL and is used for Professor Elliot's optical observing class (12.410) for upper-level undergraduates at MIT. Public tours are also available to those interested.

Although WAO is a great place for students to start observing, it also has a few disadvantages. First, it is surrounded by trees which can obstruct shed telescope observations since the trees put a higher minimum altitude constraint on observations. However, PAL members have recently looked into this situation and are working to trim these trees in order to allow for observations closer to the horizon. Second, the shed telescopes have a relatively low limiting magnitude of ~15. Third, the weather often serves as a hindrance due to seeing, atmospheric moisture and cloud cover. These factors must all be considered in any observing program. In the case of transit photometry, the choice of nights to observe is particularly limited by the occurrence of transits and the availability of brighter stars in the sky. Therefore, an up-to-date transiting planet database is necessary for any observing program doing transit photometry at WAO.

2.2   *Importance of using current planetary information*

As previously mentioned, new extrasolar planets are currently being discovered about once every other week. Astronomers not only look for new planets but also constantly take transit data on known planets in the hope of refining the physical parameters on discovered

planets. At present, papers are published every week in technical journals such as *Astrophysical Journal* and *MNRAS* with not only newly-discovered transiting planet data but also much improved data on planets that were discovered in the past twenty years. It is important to review the most recently published papers in order to prevent replicating existing data and improve our database, subsequently improving our transit prediction methods.

2.3   *PAL's database for transiting planets*

Elisabeth Adams, currently a graduate student at MIT, started PAL's database for transiting planetary parameters and their parent stars. In order to continue this database, I extracted data from the online Extrasolar Planets Encyclopaedia maintained by Jean Schneider, which is updated on a daily basis [Schneider, 1995-2008]. The website exhibits a special interactive catalog for planetary candidates detected by transit. Each planet's page shows the most recent published papers dedicated to that planet and also displays basic parameters such as right ascension α, declination δ, R_p and R_*. Typically, published papers have a characteristic set of parameters for the planet and parent star. These parameters can be seen in Figure 2 as inputs in a *Mathematica* notebook, which will be described shortly. However, some papers publish both spectroscopically-determined and photometrically-determined data. If the discrepancies between these sets of data are minute, it is standard to use the set of data with lower error bars, or the one that is more consistent with previously-published data for prediction methods.

I input these parameters into "TransitingPlanetInfo.nb," a program written in *Mathematica 5.2*, but compatible with both *Mathematica 5.2* and *Mathematica 6.0*. This notebook takes these inputs, allows the user to select which planets and parameters to output, and outputs this information to a text file. The typical input interface of this notebook can be seen in Figure 2. It also keeps track of references so the user can later verify the value of the parameter

with a specific reference paper. If transit depth and duration are not provided, the program calculates an approximate depth according to Equation 1 and duration in hours for the observer's convenience.

This program may be constantly updated so that new output text files can be used for further calculation in the accurate prediction of transits. Although astronomers have been able to detect 46 planets by transit photometry, ten of these planets have only been discovered in the last month and do not have full discovery papers with planetary parameters released yet. Therefore, the program currently has data for 36 transiting planets which are shown in Table 1 along with their celestial coordinates (α, δ). Twenty-three of these planets are candidates for transit photometry at WAO because they have positive declinations placing them high in the sky. The following section will describe our prediction method of Northern Hemisphere transits, particularly at WAO.

3 Prediction

Here I provide a list of transiting planets available for observation at WAO for both the 24-inch and 14-inch telescopes, given WAO's location and the approximate limiting magnitudes of the telescopes. I then prioritize these transits for promising projects based on magnitude, feasibility for differential photometry with promising candidates for comparison stars, and frequency of transit.

3.1 *How to computationally predict transits*

I adapted Elisabeth Adams' "PredictPotentialTransits.nb" in *Mathematica 5.2* to input transiting planetary parameters and predict when transits will occur for a given location and time period at WAO. This notebook imports the latest "TransitingPlanetInfo" text file for updated, usable planetary data. It displays relevant parameters for all planets in a table form, from which the user can select the planets of interest. The user can then input the observing location coordinates. In our case, we input WAO's latitude and longitude (see Section 2.1). WAO has a positive latitude limiting observation to the 23 transiting planets with a positive δ in the Northern celestial hemisphere. The user sets start and end dates to the prediction period. This prediction period is usually limited to a few months in order to conserve time and computing power.

The user can set many observational parameters that will help to discard unusable transits. For example, the transit could occur when the Sun is above the horizon, so the user can set a maximum solar angle that the Sun can reach below the horizon before it interferes with a transit. This constraint ensures that output transits will all occur in sufficient darkness. To ensure the planet is greater than 25° above the horizon, a maximum value for airmass, or the amount of atmosphere through which starlight passes to the Earth, can be set. In addition, since a bright, full moon can be a potent source of light pollution, the moon's apparent size and the apparent

21

distance between moon and planet are taken into consideration before the program calculates potential transits. For my runs, I set: maximum solar angle of -8° (the Sun must be 8° or more below the horizon), airmass upper limit of 2.0 (see Section 3.2), and the moon cannot come closer than 30° to the parent star of interest if the illuminated portion of the moon exceeds 85% of its full moon size (~25.5″). If the moon is farther than 30° away from the planet, it may exceed 85% of its full illumination.

The program uses the Sun, moon and planet ephemerides to determine all possible transits in the specified time period at WAO and exports the results to several text files. It exports a text file listing all full transits, a text file listing all full and partial transits, a file for the most promising transits, and a file for each of the individual planets. Table 2 lists transit output for Spring 2008 for the prediction period 01-20-2008 to 05-30-2008, which is set in the code. These are full transits and thus stages 1 through 5 should be observable for all of them (c.f. Figure 1). These data were extracted from the text file listing all full transits. For the same prediction period, an excerpt from a planet-specific text file can be seen in Figure 3, which shows both full and partial transits. Close analysis of these files is important because they reveal partial transits that may still be usable for observing. Figure 3a is an example of an unusable partial transit while Figure 3c shows an example of a usable partial transit. There are 20 transits for XO-2b alone during this prediction period, and only 4 of them are full transits, showing the significant amount of partial transits. Figure 3b shows the parameters for a full transit, which can help the user to prioritize if there happen to be multiple full transits on a given night.

In order to see whether a certain prediction period is better for transit photometry than another period, I ran the code for five different prediction periods: Fall 2007, Spring 2008, Summer 2008, Fall 2009 and Spring 2009, using the same values for airmass, solar elevation

angle, moon brightness and separation from the moon. The total number of transits, full transits, partial transits, usable and unusable partial transits for each prediction period are displayed in Table 3. Usable transits are transits during which the parameters are fulfilled >70% of the time. Table 3 also shows the percentage of usable transits out of the total number of transits during each prediction period. It is shown that the percentage of usable transits varies from ~30.00-40.00%. The fluctuation to a high percentage during the summer may be a result of the smaller sample size of days during the summer compared to the fall and spring. This relatively low percentage range of 30.00-40.00% shows that the constraints of airmass, solar angle and the moon already cut the number of total transits by more than 50%. Note that other constraints such as weather conditions or atmospheric moisture are not taken in to consideration.

The last row of Table 3 shows the highest frequency planets with full or nearly full (>90% of the time, all parameters are fulfilled) transits. This statistic excludes transits with parameters filled 90% or less of the time to show only the most reliable transiting planets. It shows that certain extrasolar planets appear to transit seasonally as viewed from WAO. For instance, the highest frequency planets during the fall of 2007 and 2008 are consistently XO-3b, WASP-1b and HAT-P-6b. Similarly, the highest frequency planets during the spring of 2007 and 2008 are HAT-P-3b, TrES-3 and XO-3b. This leads us to believe that these are the seasonally high frequency planets at WAO. This information is useful to keep in mind when creating an observing program for a certain prediction period.

3.2   *How to prioritize transits at WAO*

As previously mentioned, there are certain parameters that are important to take into consideration for observing at WAO. Since WAO's latitude is approximately 42.5° N, the most ideally located transiting planets have a positive δ of ~42.5°. These planets will be almost

directly overhead for much of the time in the Northern Hemisphere. The height of the trees also puts a restriction on the planet altitude, or angular distance from the horizon, obstructing most objects below 30° from the horizon. This translates to a maximum zenith angle z_{max} of 60° and a maximum airmass X of 2.0 since

$$z = Altitude - 30° \qquad (3)$$

$$X \cong \sec z. \qquad (4)$$

Thus, the prediction program only recognizes transits for which $1.0 < X < 2.0$.

Second, there must be one or more in-frame comparison stars in order to perform differential photometry with the parent star of interest. It is more helpful if these stars are of comparable magnitude to the star of interest in order to perform more accurate differential photometry (see Section 6.1).

Third, since the 14- and 24-inch telescopes are not extremely sensitive, they are more likely to detect a transit if the transit depth is relatively large, or >1.5% of the parent star's magnitude. This is difficult since the majority of transits range from ~0.2-3.0%. Although this factor should not prevent transit work from being done at WAO, a transit that is <1.5% will take significantly more attempts to build a successful lightcurve using WAO. The concept of taking data on successive nights to build a lightcurve is described more in Section 4.5.

3.3   *Promising candidates for Spring 2008*

Given the three factors at WAO of celestial location of parent stars, abundance of comparison stars and transit depth, I can now prioritize those full planetary transits listed in Table 2. The first aspect to consider is transit frequency, or how many times there is a full or nearly full transit for a given planet in the specified prediction period. Table 4 shows this information for Spring 2008 based on the prediction code run in Section 3.1. Since it often takes

24

multiple transits to build a successful lightcurve, planets with two or fewer transits in the specified period have been discarded. The highest frequency candidates for Spring 2008 only are HAT-P-3b, TrES-3b, XO-2b, HAT-P-5b, TrES-2 and HAT-P-4b. Table 4 also shows transit duration because this is yet another factor to consider when planning an observing program, especially for transits that may occur on the same night. It is generally easier to take data at WAO for planets with shorter transit durations since the atmospheric conditions are constantly changing and a shorter observing time reduces the potential for significant atmospheric interference.

I take a closer look at the top six high frequency transit candidates in terms of their celestial location, magnitude, available comparison stars, comparison star magnitude, angular distance from comparison star and transit depth. This information is compiled in Table 5, where the planets are ordered in decreasing frequency of transits for Spring 2008. For comparison stars, I have limited the radius of the field of view to 30″ because it is a standard value for small finderscopes and CCDs. Also, it is beneficial in photometry to have the comparison star closer to the center of the field of view to avoid limb-darkening effects in the exposures.

HAT-P-3b is a very small planet around a small parent star, although it is bright enough in comparison to its one nearby comparison star. It is the smallest planet that has been discovered photometrically, although the transit depth is still a significant 0.97% [Torres, Bakos & Kovacs et al., 2008]. The TrES-3 field has a "variety of comparison stars" and differential magnitudes can be calculated by the average weighting of these comparison stars [O'Donovan, Charbonneau & Mandushev et al., 2007]. It also has a very short period accounting for its high frequency of transit in both the spring and summer months (c.f. Table 3). The planet is quite massive compared to its host star, resulting in a strikingly large transit depth of 2.5%. XO-2b is an

excellent candidate for differential photometry because it is part of a stellar binary system, with nearby comparison star XO-2S. These two stars are also very close in magnitude (ΔV = 0.05) [Burke et al., 2007]. With a CCD field of view on the order of arcminutes such as those in the WAO shed, there is also a good comparison star west of the XO-2 binary system with V = 10.30 (c.f. Figure 4d). HAT-P-5b is an inflated, low-density planet that is a reasonably good candidate because of its abundance of proximal comparison stars and sizable 1.2% transit depth [Bakos et al., 2007]. TrES-2 has a good transit depth for detection but the area of the sky is sparse and there are not many comparison stars within a 30″ radius [O'Donovan, Charbonneau & Mandushev et al., 2007]. Lastly, HD 149026 is one of the brightest parent stars (V=8.15) with a detected transiting planet. With a large CCD field of view it is very easy to perform differential photometry on HD 149026 with a high signal-to-noise ratio because of the comparison star HD 149083 (V=8.05) that is 18′ away [Charbonneau et al., 2006]. However, this is too far for a small CCD field of view such as WAO's POETS. There are a few stars within 30″ of HD 149026 but the brightest of these are 12th and 13th magnitude. The size of the transiting planet, HD 149026b, is very small with respect to the star resulting in a very small transit depth of 0.3% [Charbonneau et al., 2006]. All of the candidates summarized in Table 3 seem promising for transit photometry at WAO except TrES-2 due to its lack of proximal comparison stars. HD 149026 will not be difficult to find due to its high magnitude but it will take a very clear night to detect the 0.3% transit dip at WAO and perform differential photometry with such faint comparison stars. TrES-3 seems to be the most promising based on its extremely high transit depth, high frequency transit, low transit duration, and availability of comparison stars.

4 Observations

4.1 *Time, weather and atmospheric considerations for transit photometry*

Although observing transits is logistically simple in that the observer points the telescope at one object for several hours, the timing of the observation is extremely important. It is important to remember to convert UTC time to EDT or EST depending on the time of year. In Boston, EST = UTC − 5 hrs from the last Sunday in October through the first Sunday in April. EDT = UTC − 4 hrs for the first Sunday in April through the last Sunday in October.

After running transit prediction codes and verifying the feasibility of the transit, it is imperative to look at not only the weather forecast but also the amount of cloud cover, atmospheric moisture, and seeing. A good resource is the WAO Clear Sky Clock, available on the WAO homepage [http://web.mit.edu/wallace]. All of these weather parameters must not interfere for at least 70% of the transit in order have a good chance of detecting the transit dip. For the shed telescopes with a limiting magnitude of ~15, the amount of cloud cover and seeing are even more important. If the forecast calls for clear skies but a high percentage of atmospheric moisture, the observer should make sure the transit is at a relatively low airmass of ~1, which translates to a nearly overhead object according to Equations 3 and 4. This will help to reduce the influence of atmospheric moisture on observation. Humidity is also an important factor, especially during the summer. Dew may collect on the telescope lens or outside of the CCD, causing unwanted interference on the exposure and damage to the equipment. Humidity is a particularly important problem when observing from the shed at WAO. Since the shed is made of wood, the building and roof expand significantly when the humidity is greater than 75% and the roof may not be able to close. These are all important to take in to consideration before conducting any observations at WAO.

4.2   *Constructing a finder chart*

I have constructed finder charts for four of the six high frequency transiting planets discussed in Section 3.3. This compilation can be seen in Figure 4a-d. These finder charts show the contrast of the sparse star field surrounding HD 149026 and HAT-P-3, to the extremely busy star field surrounding TrES-3. The binary system with XO-2 is also clearly seen in Figure 4d. These charts were constructed using the Vizier online catalog and labeled using Microsoft Powerpoint. Vizier is advantageous to use for transit photometry because it combines many star databases so that the best comparison stars available can be found. However, the Aladin images supplied by Vizier are generally at least 13' by 13'. In the case of a small CCD field of view, these finder charts would only be good for finding the star because the image is representative of a typical finderscope field of view, but it might not be ideal for finding comparison stars within the CCD field of view. The Vizier database also has so many stars that it can sometimes get overwhelming at the telescope to identify the correct parent star of interest. Starry Night Pro™ is a much simpler but less comprehensive program to construct finder charts. However, Starry Night's database is much less extensive than that of Vizier and therefore may not show all potential comparison stars.

4.3   *Typical observing plan for a transit at WAO*

Transit photometry is ideal at large telescopes with efficient automated tracking such as the 24-inch telescope at WAO. Transits generally last a minimum of 1.5 hours (c.f. Table 4) with an additional one hour before and after the transit itself in order to obtain the baseline magnitude of the parent star and ensure a high signal-to-noise ratio on these exposures. It is therefore useful to have tracking so the user does not need to manually reposition the telescope during the transit. Since the output lightcurve will ultimately depend on the detection of the dip, it is important to

take as many exposures as possible during the transit, stage 2 through stage 4 (c.f. Figure 1), at evenly-spaced time intervals. For stage 1 and stage 5, it is less imperative to take a large amount of exposures, since one does not expect the differential magnitude of the parent star to change. A typical transit observing plan for TrES-3, which has a transit duration of 1.4 hours and $V = 12.4$, is shown in Table 6 on a telescope with automated tracking and frame-transfer capability. As mentioned in Section 2.1, frame-transfer capability enables a CCD to take an exposure almost simultaneously as it reads out the previous frame. Therefore, readout time is negligible and does not need to be included in the calculation. Since TrES-3 has a very short transit duration, the observer could afford to shorten stage 1 and stage 5 to 30 minutes. However, I have included an hour of time before and after the transit to ensure this high signal-to-noise ratio regardless of the parent star's magnitude. Dark calibration frames should be taken at the beginning and end of the night to match the exposure time length and filters of the transit observations. Bias calibration frames should be taken at these times as well. Typically, these calibration frames are also taken in the middle of an observation run but it is not advisable during transit photometry since it would interrupt the transit. A more detailed description of calibration frames is in Section 5.1.

In order to calculate the exposure time needed, it is important to consider the star's magnitude, potential saturation by any in-frame object or the star itself, and the limiting magnitude of the telescope. Typically, exposure times for transits will range between 30 seconds and 2.5 minutes depending on the sensitivity of the CCD. The exposure time should be set prior to stage 1 of the transit, so be sure to include this in total observation time. The exposure time used in Tables 6 and 7 is arbitrary based on past experience at WAO with photometry of objects similar in magnitude.

For telescopes with less reliable tracking such as the shed telescopes at WAO, the observation plan must be altered. This altered plan is shown in Table 7. First, these CCDs do not have frame-transfer capability so an exposure must be read out before the next exposure can be taken. From experience, the readout time at WAO increases approximately linearly with increasing exposure length. Thus, the highest available frequency of exposure is much lower for CCDs with frame-transfer capability. Second, the user must look through the eyepiece of the telescope every so often to ensure that the parent star is still in the CCD frame. A safe estimate is every 10 minutes, for a maximum of 30 seconds each time. Table 7 also takes this into account for the total available exposure time during the transit. Lastly, the sensitivity of the CCD is significantly lower on these shed telescopes and thus it is more difficult to achieve a comparable signal-to-noise ratio to that of the POETS CCD. In order to achieve a high signal-to-noise ratio, the frequency of exposure must be increased to a maximum rate of one exposure for every two minutes for the entire transit, including stages 1 and 5. CCDSoft^{TM} allows the user to automatically take sets of consecutive exposures at evenly-spaced time intervals to help this process.

4.4   *What to do on a clear night when there is no transit*

If there is a clear night but no transit at WAO, it is important to take advantage of this night to obtain solid baseline data. The observer should prepare a list of transiting planets that are expected for the observing program along with their finder charts. It is then useful to take data on each of the parent stars in the absence of a transit. These data can later be used to achieve a higher signal-to-noise ratio and reduce residuals for the baseline magnitude of the star on a subsequent transit lightcurve if needed. It will also allow the observer to target any good comparison stars in the CCD frame. Any experience with setting up the telescope and pointing it

to the parent star will minimize the stress of finding the object, locating comparison stars and figuring out the exposure time needed when the actual transit comes.

4.5   Advantages of composite lightcurves

Completely clear skies are rare in many parts of the world, including Boston. Often observers will start to perform transit photometry and become clouded out by stage 4. Therefore, it may be helpful to combine data on the same extrasolar planet from multiple nights in order to get a complete lightcurve. This is one advantage of using multiple comparison stars in differential photometry, since these comparison stars will eliminate most atmospheric fluctuations from night to night. However, it is nearly impossible to combine data taken months apart. Figure 5 shows when candidates transit for the Spring 2008 prediction period over time. This figure gives an idea for the best planetary candidates for composite lightcurves for the Spring 2008 prediction period based on which planets have nearly consecutive transits.

4.6   Observations for XO-2b transit on 03-25-2008 UTC

Extrasolar planet transit data at WAO was taken for the first time using the POETS CCD on the 24-inch telescope by Matthew Lockhart, a current graduate student with PAL at MIT. The extrasolar planet was XO-2b, transiting parent star XO-2 starting the night of 03-24-08 in EST, or the morning of 03-25-2008 in UTC.

The weather conditions were conducive to observing, with a temperature of 36° F, no precipitation, and few clouds in the sky. XO-2 was projected to be in an airmass range of 1.01 to 1.33 for the transit. Using Equation 4, we find that the zenith range is ~70°-90°, with XO-2 stage 2 starting at 90°. Therefore, we would expect the seeing to become slightly worse throughout the transit. Toward the end of the observing session, the seeing was indeed reported to be significantly worse than in the beginning. The moon was expected to reach a high level of 90.3%

of its full illumination during the transit. However, it was 119° away from XO-2, so it should not have interfered greatly with the observed transit (c.f. Table 8).

The transit mid-time (stage 3) was predicted to occur at 02:04:56 UTC. XO-2b has a transit duration of approximately 2.6 hours (c.f. Table 4), so this transit was expected to start (stage 2) at 00:28:56 UTC and end (stage 4) at 03:40:56 UTC. Therefore, an observation of all five stages of the transit would require open-shutter observations to start one hour before stage 2, around 23:28:56 UTC and end one hour after stage 4, around 04:40:56 UTC. However, transit red filter observations only began at 00:43:40 UTC and ended at 03:43:20 UTC. With this data, we would expect to see the end of stage 2 when the dip starts, to the beginning of stage 4 when the dip retains a baseline level on the lightcurve.

The POETS CCD field of view allows for differential photometry with XO-2S but no other star of comparable magnitude (c.f. Figure 4d). Thus, this set of exposures is not ideal for effective differential photometry. Several exposure times were tested before settling on an individual exposure length of 140 seconds. A set of preliminary 80-second exposures were tested with the telescope's clear filter but the data saturated very easily which would result in unusable transit data. Therefore, the telescope's red filter was used for all open-shutter observations and a high signal-to-noise ratio was achieved without image saturation.

75 open-shutter red filter frames, each 140 seconds long, were taken throughout the night, resulting in four FITS data cubes. Around stage 3, there was a severe shift of the CCD frame half a frame to the west knocking the target nearly off of the frame. However, there appeared to be no such shift in the telescope's finder. Shortly thereafter, the finder image started to vibrate resulting in exposures with streaky objects. Data-taking was not stopped during this time, so 19 of the 75 red filter frames were unusable in data reduction due to this severe shift of the CCD. The target

was re-centered after that set of images was taken so the beginning of stage 4 could still be seen.

15 140-second dark frames and 15 0-second bias frames were taken at the end of the night, and

all calibration frames were used in data reduction.

5 Data Reduction

5.1 *Data calibration for the CCD*

There are three types of calibration for CCD exposures. The first is dark current calibration which corrects for the thermal noise of the CCD. This noise increases with exposure length so the length of the dark calibration images must equal the length of each exposure. If multiple exposure lengths are used, multiple dark calibration images must be taken. These dark calibration images are ultimately subtracted from the open filter exposures.

The second type of calibration is bias calibration. These are dark current exposures with a zero-second exposure time when the shutter is closed. Bias frames correct for the intrinsic readout noise of the CCD and any other general noise from the electronics. Both bias and dark frames should be taken at the beginning, middle and end of the night. These bias frames are ultimately subtracted from the open filter exposures.

The third type of calibration is the flat field calibration. These frames correct for the difference in the CCD's sensitivity to light from pixel to pixel. Flat field frames should be taken either on a completely uniform sky, typically just before twilight, or on a uniform surface such as a white board. Like dark current exposures, flat field exposures should be taken to match each length of the open filter exposures. Open filter exposures are ultimately divided by these flat frames during data calibration.

5.2 *Calibrating data for analysis with IDL using phot*

In order to access data at WAO, exposures are transferred from the WAO shed computer to the server TITANIA_EXT_A on the observatory's data archive computer after all exposures are taken on any given night. The data are then transferred from TITANIA_EXT_A to the MIT Athena server.

IDL, or Interactive Data Language, is a software package available to all MIT students on the Athena server. In addition to having simple dark, bias and flat calibration methods, it also contains the *phot* routine which takes a list of calibrated CCD images and outputs many useful parameters such as an object's photon counts with and without the background counts, the time of each exposure, and the standard deviation of the background counts in the exposure. It allows the user to click on an astronomical object and the sky background in any given exposure forming boxes around each of the regions. Typical box sizes for a point source are 30 square pixels but the user may adjust the box size according to the size of the object of interest. It then takes the object's total number of photon counts S within the first box and subtracts the total number of background counts B within the second box. This parameter $S-B$ is essentially the number of counts from the object alone without any extraneous counts from the sky background. In the case of transit photometry, it is very important to have this number of photon counts of the parent star alone in order to build an accurate lightcurve. Also, as previously mentioned all objects used for data analysis should not be near the edge of the frame, since the edge of the CCD tends to distort the image and will therefore distort the results.

The IDL routine *phot* also allows the user to perform box photometry on multiple objects in a single field. This is useful for in-frame comparison stars whose $S-B$ values are used in subsequent calculations in order to perform differential photometry. Having completed these data reduction calibration steps in IDL, the data is now in a usable form for analysis.

5.3   *Preparing data for analysis with Mathematica 6.0*

The above calibration through IDL may be bypassed if the "Make_Lightcurve.nb" program is used for data analysis. This *Mathematica* notebook, further described in Section 6.2, calibrates the data, performs differential photometry and outputs usable numbers to construct a

lightcurve all in one program. It is specifically designed to read in the FITS data cubes output by

POETS. Therefore, it is the primary notebook used for data analysis in this thesis.

6 Results & Data Analysis

6.1 *Steps for calculating differential magnitude*

Before diving in to the computational aspect of transit data analysis, it is important to understand mathematically how differential photometry is performed using in-frame comparison stars to calculate a differential magnitude of the target object. This differential magnitude takes into account and corrects for any intrinsic variability in the telescope or atmosphere at a certain time of night. I provide a brief mathematical basis on how to calculate the differential magnitude using WAO data, since the assumed information can be easily extracted from the FITS file with the standard IDL calibration routines *makedark, makebias, multiccdproc* and *phot*. These routines are described in Susan Kern and Professor Elliot's laboratory manual for the optical observational astronomy class 12.410 [Kern & Elliot, 2007]. Calculating the differential magnitude requires information from both the target star and any in-frame comparison stars.

The first step in analysis is to calculate the instrumental magnitude of each of the astronomical objects in every frame: the parent star, and any number of comparison stars. Here, we will arbitrarily name two comparisons Star 1 and Star 2. The formulas for instrumental magnitude m_i and its variance $\sigma^2(m_i)$ are given by

$$m_i = -2.5 \log\left(\frac{S-B}{T}\right) \tag{5}$$

$$\sigma^2(m_i) = \left(\frac{\partial m_i}{\partial(S-B)}\right)^2 = \left(-2.5\left(\frac{1}{\ln 10}\frac{1}{(S-B)}\right)\right)^2 \sigma^2(S-B), \tag{6}$$

where $S\text{-}B$ is the background-subtracted object count, T is the integration time, and $\sigma^2(S\text{-}B)$ is given by the square of the box size enclosing the object multiplied by the square of the standard deviation per pixel output. The error can be approximated as the square root of the variance, or

the standard deviation. These formulas are not filter-specific allowing for transit photometry in any desired filter.

The next step is to obtain the differential magnitude by subtracting the instrumental magnitude of the comparison stars from the instrumental magnitude of the parent star. Ideally, the average instrumental magnitude of the comparison stars would be subtracted from the instrumental magnitude if both comparison stars were of comparable instrumental magnitude to the parent star. However, if it is the case that Star 1 is significantly closer in instrumental magnitude to the parent star than Star 2, only Star 1 is used. The general formula for the differential magnitude m_d of the parent star and its variance $\sigma^2(m_d)$ are given by

$$m_d = m_{i_{ParentStar}} - \frac{\left(m_{i_{Star1}} + m_{i_{Star2}}\right)}{2} \tag{7}$$

$$\sigma^2(m_d) = \sigma^2(m_{i_{ParentStar}}) + \sigma^2(m_{i_{avg}}) \tag{8}$$

With this differential magnitude m_d calculated for each frame, the transit data taken have now undergone complete differential photometry and are ready to be used for a lightcurve.

6.2   *Computational analysis of transit data*

The *Mathematica* notebook "Make_Lightcurve.nb" is used for making lightcurves of transit data. The notebook works well with WAO data because it performs all of the bias, flat and dark calibration for the user straight from the raw FITS files output from the CCD. Therefore, the user does not have to go through IDL's calibration routines in order to correctly calibrate the data. Second, the notebook uses the simple mathematical equations described in Section 6.1 in order to calculate differential magnitude. It also allows the user to specify different box sizes for the parent star and comparison stars as well as visualize the frame while running the code. It then takes the calculated values and either plots the differential magnitude of the parent star over time and exports a lightcurve, or outputs the numbers for differential magnitude and time so the user

38

can use these to plot in an alternate graphing program. However, this notebook is intensive in computing power but is simpler than using IDL routines and then having to use an additional graphing program.

6.3   *XO-2b transit data*

I reduced the observational data of the XO-2b transit, described in Section 4.6, with "Make_Lightcurve.nb" in *Mathematica 6.0*. There were 75 open-shutter frames total resulting in four FITS data cubes with three sets of 15 frames and one set of 30 frames. As previously mentioned, 19 of these frames turned out to be unusable. For the first frame in the first data cube, I used a box size of 375 x 375 pixels with origin (x,y) at (100, 100) to encompass XO-2, XO-2S and the background. The box for XO-2 was centered at (228, 300) while the box for the comparison star XO-2S was centered at (254, 220). The background box was centered at (150, 150). Each of these three boxes was 35 x 35 pixels. These values remained relatively constant throughout the data reduction of this transit.

I ran the program once for each data cube to ensure that there had been no large shifts of the CCD in between sets of frames. I compiled the results of each frame into one lightcurve and plotted the differential magnitude against hours in UTC. The results are shown in Figure 6.

There is a defined, prolonged dip from 01:12:00 UTC to 03:30:00 UTC. This translates into a transit duration of 2.3 hours. The gap between 01:40:00 UTC and 02:24:00 UTC is explained by the lack of usable data from the shifting of the POETS CCD. The worsened seeing reported toward the end of the transit may account for the more uneven data around stage 4.

39

7 Conclusions & Future Work

7.1 *WAO transit capabilities on the 24-inch telescope*

The partial transit shown in Figure 6 is promising for the feasibility of transit photometry at WAO. Although no baseline magnitude for the parent star XO-2 was obtained, Figure 6 shows that WAO can detect minute but defined dips given the correct weather conditions. One other transit has been observed in Spring 2008, although extremely bad seeing conditions were reported for half of the transit rendering the data almost useless. The April 2008 transits are listed in Table 8 along with their observing conditions as output by the prediction code. If the transit was not observed, a reason is stated for why it was not observed. It can be seen that obtaining a lot of transit data is difficult but doable in one month, although this is highly dependent on the availability of the observer and the weather conditions for that month. Figure 6 suggests that the POETS CCD on the 24-inch telescope can detect full transits, so PAL's observing program at WAO should be able to launch smoothly.

7.2 *An efficient planetary database and prediction method*

I have outlined PAL's extrasolar planetary database and prediction method. These aspects are not only easy to learn, but the files also exist in one place on the lab's server so that any student should be able to pick up the project easily without having to transfer files from computer to computer. Since we recently launched our program in Spring of 2008, there have only been a few attempts of taking transit data at WAO. We have formed a solid formulaic method for creating a transit photometry observing plan for any prediction period in the near future at WAO so that we are ready to take data with both the 24-inch and the shed telescopes.

7.3 *WAO shed upgrade yields more transit photometry capabilities*

The CCDs on shed telescopes 3 and 4 have recently undergone a large upgrade from SBIG ST-237A to SBIG STL-1001E. The main difference is the much larger CCD field of view. This CCD field of view should allow for a higher chance of better differential photometry due to the greater potential for good in-frame comparison stars. Although the telescope itself is the same and therefore the limiting magnitude will remain unchanged, the CCD sensitivity is much higher and it will be easier to obtain a high signal-to-noise ratio even at the telescope's limiting magnitude of ~15.

This upgrade will only help to ensure the feasibility of transit photometry at WAO. With a solid observing plan and a good method for prioritizing transits, the project should be feasible on the shed telescopes at WAO. Successful transit photometry on the shed telescopes would be exciting to share with the astronomical community because published transits are typically performed on large telescopes and rarely on telescopes under 0.5 m. With the data presented in this thesis as well as the thorough PAL database, prediction methods and observing plans, avid students are encouraged to take on a semester-long transit photometry project at WAO.

8 References

Bakos G, Shporer A, Pal A, Torres G, Kovacs G, Latham D, Mazeh T, Ofir A, Noyes R, Sasselov D, Bouchy F, Pont F, Queloz D, Udry S, Esquerdo G, Sipocz B, Kovacs G, Lazar J, Papp I, Sari P. ApJ, Letters. 671: L173-L176. (2007). "HAT-P-5b: A Jupiter-like hot Jupiter Transiting a Bright Star."

Burke C, McCullough PR, Valenti JA, Johns-Krull CM, Janes KA, Heasley JN, Summers FJ, Stys JE, Bissinger R, Fleenor ML, Foote CN, Garcia-Melendo E, Gary BL, Howell PJ, Mallia F, Masi G, Taylor B, Vanmunster T. ApJ. 671: 2115-2128. (2007). "XO-2b: Transiting Hot Jupiter in a Metal-rich Common Proper Motion Binary."

Charbonneau D, Winn JN, Latham DW, Bakos G, Falco EE, Holman MJ, Noyes RW, Csak Balazs, Esquerdo GA, Everett ME, O'Donovan FT. ApJ. 636: 445-452. (2006). "Transit Photometry of the Core-Dominated Planet HD 149026b."

Gulbis AAS, Elliot JL, Person MJ, Babcock BA, Pasachoff JM, Souza SP, Zuluaga CA. AIP Conf. Proc. 984: 91-100. (2008). "Recent Stellar Occultation Observations Using High-Speed, Portable Camera Systems."

Hartmann, WK. Moons & Planets. 5 ed. Brooks/Cole. (2005).

Kern, S & Elliot JL. Lab Manual for 12.410J-8.287J. Updated 2007 Sept 5.

Kovacs G, Bakos GA, Torres G, Sozzetti A, Latham DW, Noyes RW, Butler RP, Marcy GW, Fischer DA, Fernandez JM, Esquerdo G, Sasselov DD, Stefanik RP, Pal A, Lazar J, Papp I, Sari P. ApJ. 670: L41-L44. (2007). "HAT-P-4b: A Metal-rich Low-Density Transiting Hot Jupiter."

Latham DW, Stefanik RP, Mazeh T, Mayor M, Burki G. Nature. 339: 38-40. (1989). "The unseen companion of HD 114762 – A probable brown dwarf."

Li C, Benedick AJ, Fendel P, Glenday AG, Kartner FX, Phillips DF, Sasselov D, Szentgyorgyi A, Walsworth R. Nature. 452: 610-612. (2008). "A laser frequency comb that enables radial velocity measurements with a precision of 1 cm s^{-1}."

Mayor M & Queloz D. Nature. 378: 355-399. (1995). "A Jupiter-mass companion to a solar-type star."

MIT Planetary Astronomy Lab. <http://occult.mit.edu/index.php>.

O'Donovan FT, Charbonneau D, Bakos GA, Mandushev G, Dunham EW, Brown TM, Latham DW, Torres G, Sozzetti A, Kovacs G, Everett ME, Baliber N, Hidas MG, Esquerdo GA, Rabus M, Deeg HJ, Belmonte JA, Hillenbrand LA, Stefanik RP. ApJ. 663: L37-L40. (2007). "TrES-3: A Nearby, Massive, Transiting Hot Jupiter in a 31-Hour Orbit."

O'Donovan FT, Charbonneau D, Mandushev G, Dunham EW, Latham DW, Torres G, Sozzetti A, Brown TM, Trauger JT, Belmonte JA, Rapus M, Almenara JM, Alonso R, Deeg HJ, Esquerdo GA, Falco EE, Hillenbrand LA, Roussanova A, Stefanik R, Winn JN. ApJ. 651: L61–L64. (2007). "TrES-2: The First Transiting Planet in the *Kepler* Field."

Schneider J. The Extrasolar Planets Encyclopaedia. 1995-2008. <http://exoplanet.eu>.

Seager S & Mallén-Ornelas G. ApJ. 585: 1038-1055. (2003). "A Unique Solution of Planet and Star Parameters from an Extrasolar Planet Transit Light Curve."

Software Bisque. 2004-2007. <http://www.bisque.com/>.

Souza SP, Babcock BA, Pasachoff JM, Gulbis AAS, Elliot JL, Person MJ, Gangestad JW. PASP. 118: 1550-1557. (2006). "POETS: Portable Occultation, Eclipse, and Transit System."

Space Inferometry Mission PlanetQuest. <http://planetquest.jpl.nasa.gov/SIM/sim_index.cfm>.

Torres G, Bakos GÁ, Kovács G, Latham DW, Fernández JM, Noyes RW, Esquerdo GA, Sozzetti A, Fischer DA, Butler RP, Marcy GW, Stefanik RP, Sasselov DD, Lázár J, Papp I, Sári P. ApJ. 666: L121-124. (2008). "HAT-P-3b: A Heavy-Element-Rich Planet Transiting a K Dwarf Star."

Torres G, Winn JN, Holman M. ApJ. 677: 1324-1342. (2008). "Improved Parameters for Extrasolar Transiting Planets."

Udalski A, Szymanski M, Stanek KZ, Kaluzny J, Kubiak M, Mateo M, Krzeminski W, Paczynski B & Venkat R. ACTA Astronomica. 44: 165-189. (1994). "The Optical Depth to Gravitational Microlensing in the Direction of the Galactic Bulge."

VizieR service online catalog. VizieR Service at Centre de Données astronomiques de Strasbourg. <http://130.79.128.14/viz-bin/VizieR>.

Wallace Astrophysical Observatory. <http://web.mit.edu/wallace>.

Appendix 1   Figures
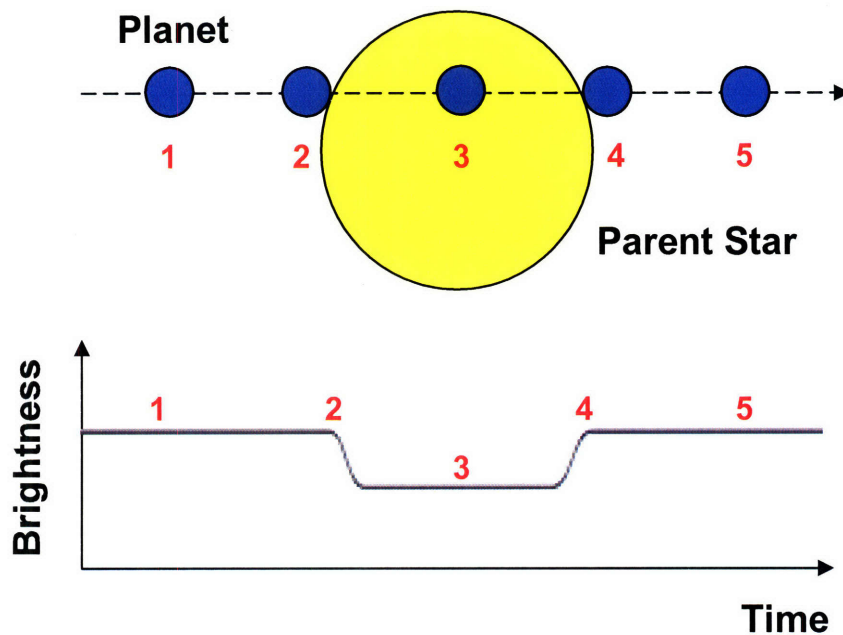
Planet

Figure 1. Primary extrasolar planet transit and corresponding lightcurve schematic. This schematic shows the five stages of a typical extrasolar planet transit and the corresponding points on the photometric lightcurve of the parent star. Although we cannot physically see the planet, we know that as it transits its parent star, it marginally blocks incoming light from the star and decreases the star's magnitude (~0.2-3.0%) depending on the relative sizes of the star and planet. This transit results in a wide, shallow dip, starting at stage 2 (ingress) when the planet is about to transit the star and ending at stage 4 (egress) when the planet has just finished. Although stages 1 and 5 occur well before and after the actual transit, it is important to take baseline photometric data at these stages in order to ensure detection of the transit itself since the reduction in magnitude is so small. It is often sufficient to take photometric data for stages 1-3 only and extrapolate the remaining lightcurve assuming a symmetrical dip over time. We look for this characteristic dip in our detection of extrasolar planets.

■ Best values (use this section)

```
planet = "TrES-3";
mass[planet] = "1.92"; (* Mjup *)
massErr[planet] = "0.23";
radius[planet] = "1.295"; (* Rjup *)
radiusErr[planet] = "0.081";
period[planet] = "1.30619"; (* days *)
periodErr[planet] = "0.00001";
transitTime[planet] = "4185.9101"; (* HJD - 2450000 *)
transitTimeErr[planet] = "0.0013";
inc[planet] = "82.15"; (* degrees *)
incErr[planet] = "0.21";
aAU[planet] = "0.0226"; (* AU *)
aAuErr[planet] = "0.0013";
starRA[planet] = "17 52 07.03";
starDec[planet] = "37 32 46.1";
starRadius[planet] = "0.802"; (* Rsun *)
starRadiusErr[planet] = "0.046";
starMass[planet] = "0.90"; (* Msun *)
starMassErr[planet] = "0.15";
starMagV[planet] = "12.402";
starMagI[planet] = "11.603";
starMagJ[planet] = "11.015";
starDistance[planet] = "NA"; (* parsec *)
starU1[planet] = "NA";(* limb darkening: 1-u1*(1-mu)-u2*(1-mu)^2 *)
starU2[planet] = "NA"; (* limb darkening: 1-u1*(1-mu)-u2*(1-mu)^2 *)
starTemp[planet] = "5720";
transitDepth[planet]="2.5%";
radiusRatio[planet]="0.1660";
radiusRatioErr[planet]="0.0024";

refsUsed[planet] = {"ODononvan2007"};
refNotes[planet] = "Discovery paper.";
```

Figure 2. "TransitingPlanetInfo.nb" input interface example. This is an example of the *Mathematica* interface where the user may input any of the above parameters with the units indicated. The program will then take these parameters, output them to a text file, and use the text file for transit prediction. The above example is TrES-3. "NA" indicates that no parameter is being input. Strings are used instead of numbers in order to preserve decimal point accuracy without normalizing all numbers to a certain number of places.

```
Site (lat, long)        Wallace (42 36 36.0, -71 29 06.0)
Search dates            2008 01 20 00 00 00 to 2008 05 30 00 00 00
Airmass cutoff          2.
Solar alt limit (deg)   -8.
Closest moon (deg)      30.
Pad each side (hrs)     1.


PLANET                  XO-2b
Period                  2.615838000
RA                      7 48 6.47
Dec                     50 13 33.
Duration (hrs)          2.6328
In partial schematics below, each 'x' or '-' represents 5. minutes
```
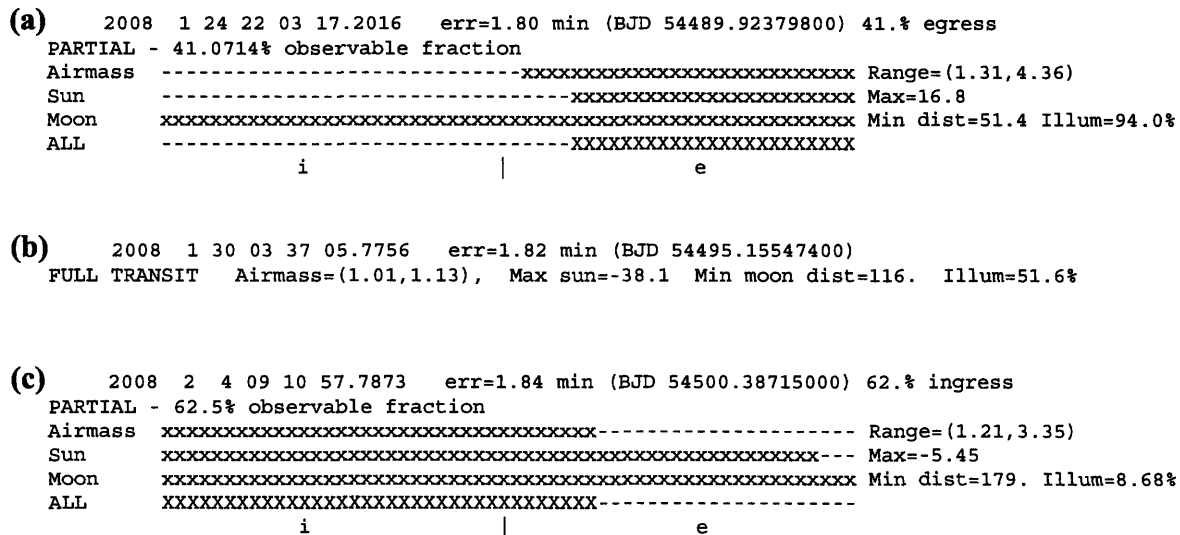
```
(a)    2008  1 24 22 03 17.2016   err=1.80 min  (BJD 54489.92379800)  41.% egress
       PARTIAL - 41.0714% observable fraction
       Airmass  ------------------------------xxxxxxxxxxxxxxxxxxxxxxxxxxx Range=(1.31,4.36)
       Sun      -------------------------------xxxxxxxxxxxxxxxxxxxxxxxxxx Max=16.8
       Moon     xxxxxxxxxxxxxxxxxxxxxxxxxxxxxxxxxxxxxxxxxxxxxxxxxxxxxxxxxx Min dist=51.4 Illum=94.0%
       ALL      -------------------------------XXXXXXXXXXXXXXXXXXXXXXXX
                            i                  |            e
```

```
(b)    2008  1 30 03 37 05.7756   err=1.82 min  (BJD 54495.15547400)
       FULL TRANSIT   Airmass=(1.01,1.13),  Max sun=-38.1  Min moon dist=116.  Illum=51.6%
```

```
(c)    2008  2  4 09 10 57.7873   err=1.84 min  (BJD 54500.38715000)  62.% ingress
       PARTIAL - 62.5% observable fraction
       Airmass  xxxxxxxxxxxxxxxxxxxxxxxxxxxxxxxxxxxx-------------------- Range=(1.21,3.35)
       Sun      xxxxxxxxxxxxxxxxxxxxxxxxxxxxxxxxxxxxxxxxxxxxxxxxxxxxxxx--- Max=-5.45
       Moon     xxxxxxxxxxxxxxxxxxxxxxxxxxxxxxxxxxxxxxxxxxxxxxxxxxxxxxxxxxx Min dist=179. Illum=8.68%
       ALL      XXXXXXXXXXXXXXXXXXXXXXXXXXXXXXXXXXXX--------------------
                            i                  |            e
```

Figure 3. Excerpt from text file for XO-2b Spring 2008 transits. This is an example of the output from "PredictPotentialTransits.nb" for a single planet. The file header provides all useful input information. The program was run for WAO transits from 01-20-2008 to 05-23-2008, with observational parameters set as mentioned in Section 3.1. The header lists basic information such as planet name, α, δ and duration of transit. (a) Here is a partial transit. The four observational parameters are only met for ~41% of the transit. The top line indicates the date of transit (YYYY MM DD) and start time in UTC. Consider the horizontal axis to be time, where each "-" or "x" denotes 5 minutes and "i", "|" and "e" stand for stage 2 (ingress), stage 3, and stage 4 (egress) respectively. The three parameters airmass, sun and apparent distance from moon are listed on the vertical axis. A "-" indicates that that user-specified parameter is not met, while an "x" indicates that it is met. For instance, if a "-" appears in the "Sun" row, this means that the Sun is above the -8° limit for that timepoint. Looking at the entire transit, useful observing can only occur for 34.8% of the actual transit (55/157 minutes), and one needs at least 70% to get an acceptable lightcurve. (b) This figure shows a predicted full transit, where all parameters are met for the entire period. The date and time of transit are shown. The airmass, maximum solar angle, minimum moon distance and moon illumination are listed. If the user finds multiple transit possibilities for one night, he may prioritize based on % moon illumination or timing. (c) This figure shows a partial transit that may be reasonable to observe since all parameters are met for 62.5% including the transit and one hour of observing time beforehand. The moon is only 8.68% full, while the Sun and Moon requirements are met past egress.
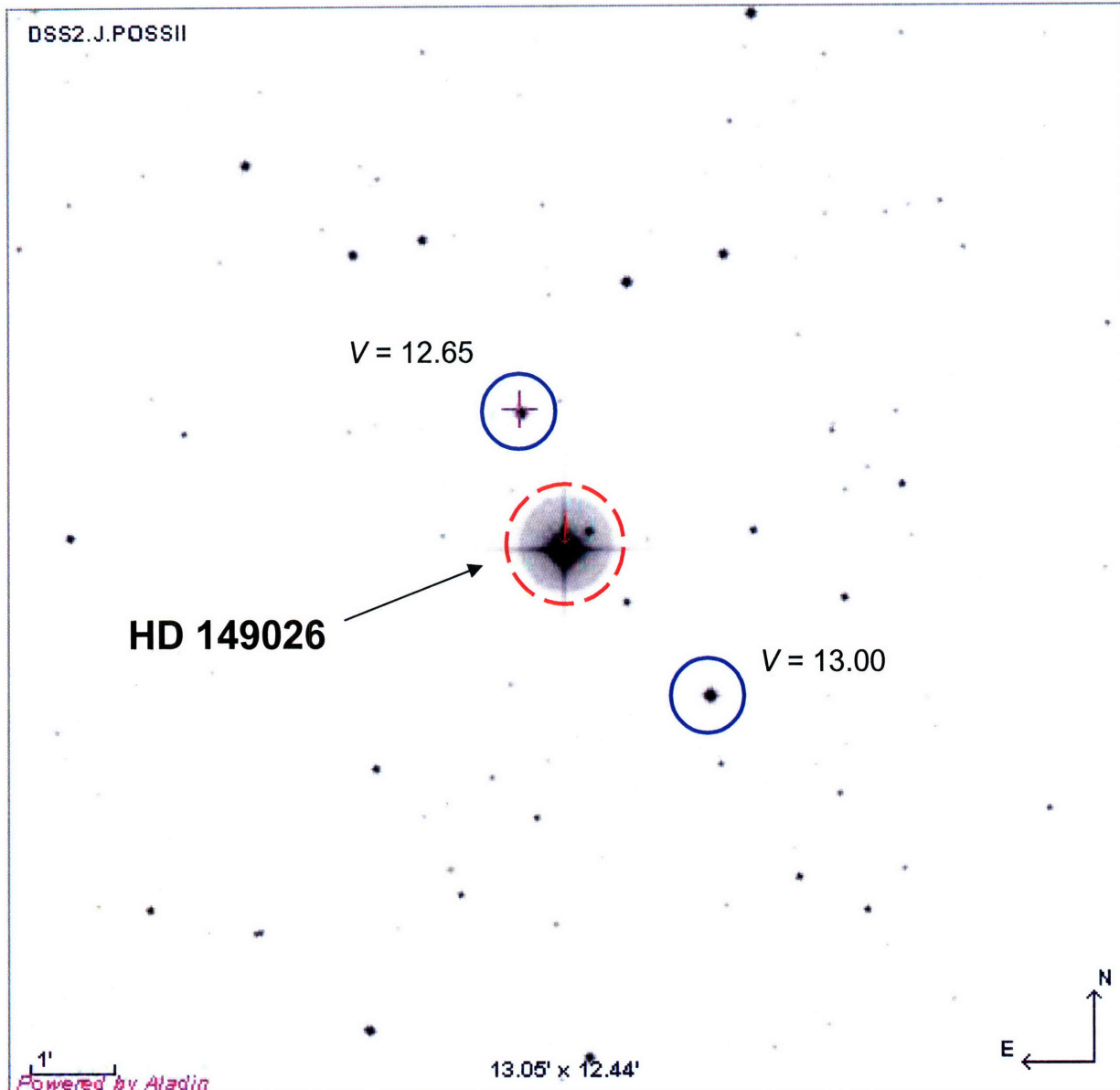
(a)

Figure 4. Finder charts for four high frequency transiting planets for Spring 2008. These finder charts were made using Vizier online service by inputing the α and δ of each parent star of interest (c.f. Table 1) and downloading an Aladin image for each parent star. The text and circular region overlays were created in Microsoft Powerpoint. Red dotted circles in the center of each image indicate the parent star of interest, while blue solid circles represent good comparison stars for differential photometry. The magnitudes provided are from the catalog. The image scale of each is depicted on the bottom left and the celestial axes are on the bottom right. **(a)** This is a 13.05′ by 12.44′ Aladin image centered on HD 149026 from the Guide Star Catalog (GSC). *V* magnitudes of two good candidate stars are provided. Notice that there are a few very faint stars in the immediate vicinity of HD 149026 but these are of magnitude *V* ~ 17 and would not be as good for differential photometry if the CCD FOV is large enough to encompass the circled stars.
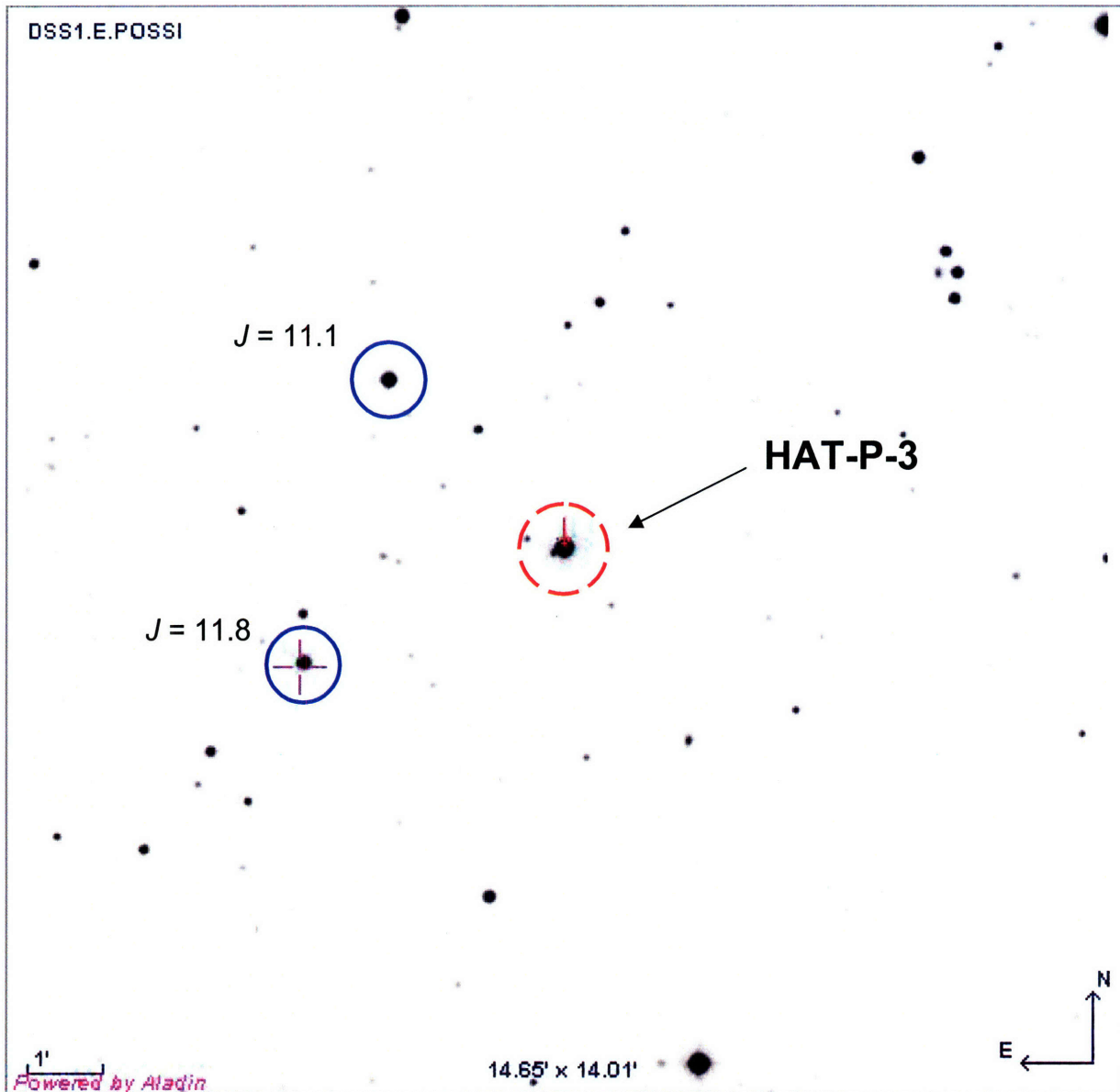
(b) This is a 14.65′ by 14.01′ Aladin image centered on HAT-P-3 from the 2MASS star catalog. *J* magnitudes of two good candidate stars are provided. Notice the relative abundance of bright stars in this field. The closest and brightest have been labeled, but since HAT-P-3 is only $V \sim 11$, faint, closeby stars may be used for differential photometry as well.
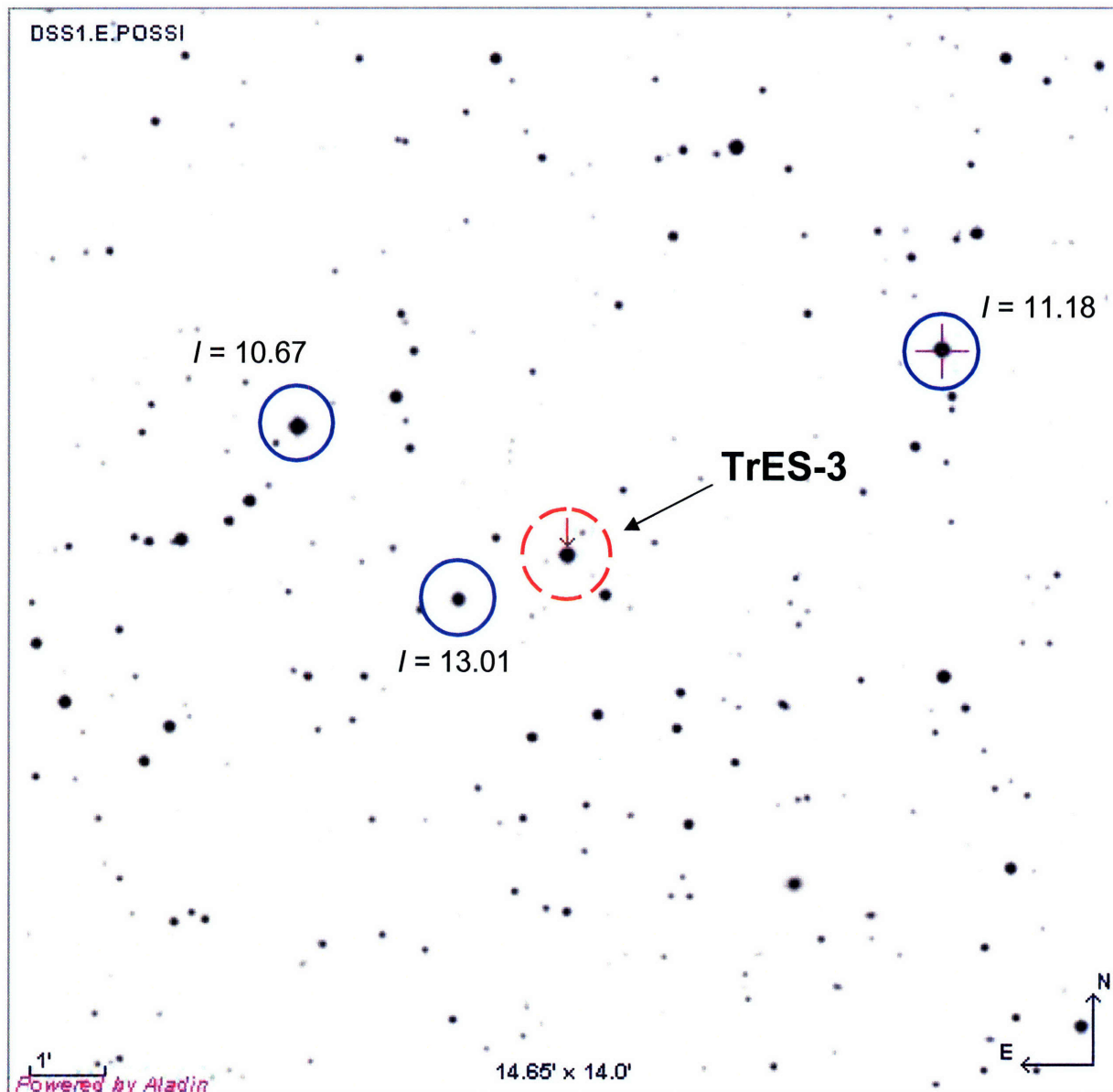
(c) This is a 14.65′ by 14.0′ Aladin image centered on TrES-3 from the United States Naval Observatory (USNO) star catalog. As mentioned in O'Donovan et al. (2007), there is an abundance of stars in this field [O'Donovan FT, Charbonneau D & Bakos GA et al., 2007]. Three of the brightest stars in this field have been labeled with their *I* magnitudes. With a much smaller CCD FOV, any nearby star, even those just outside the central dotted red circle, would be sufficient for differential photometry.
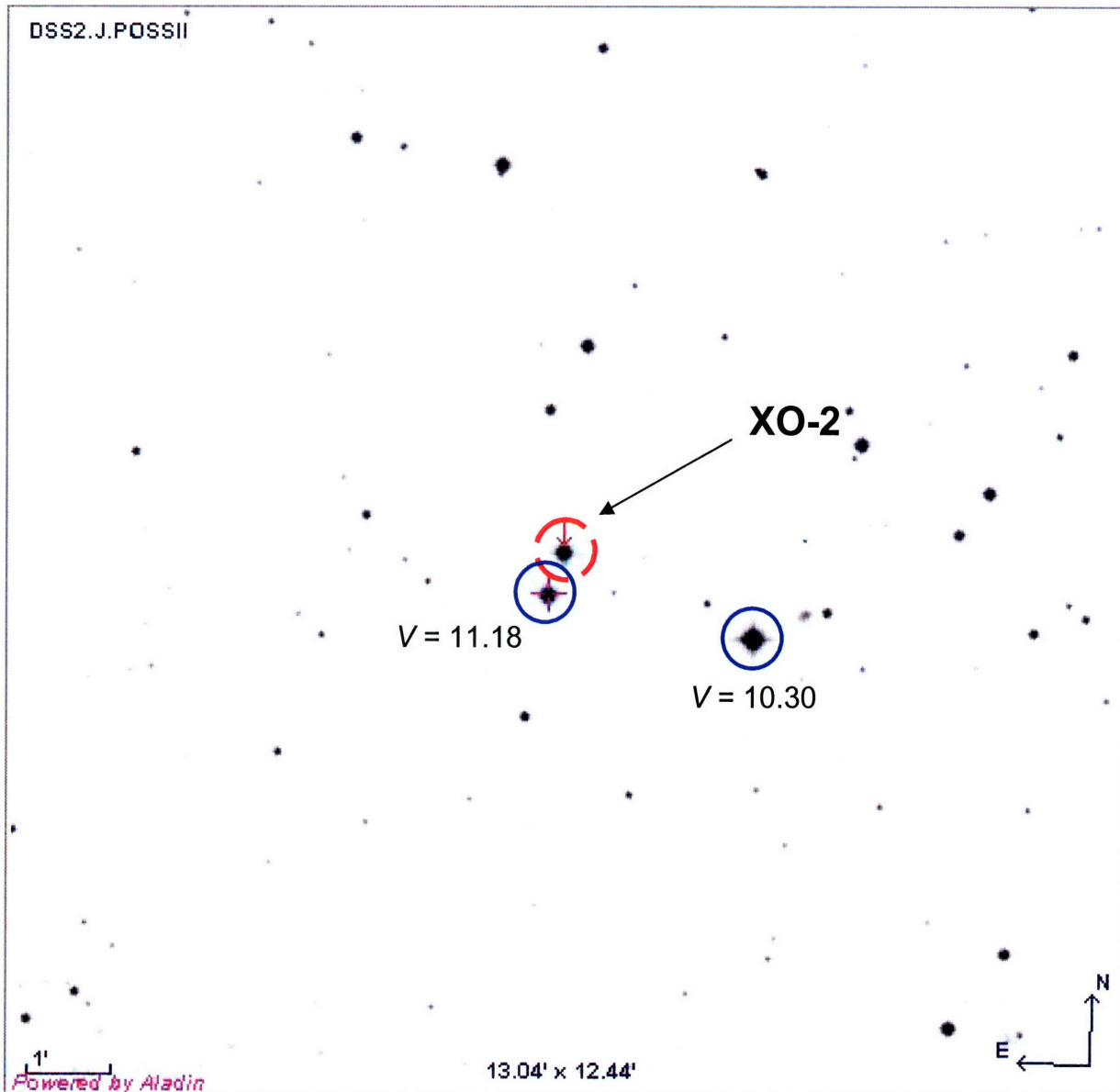
(d) This is a 13.04′ by 12.44′ Aladin image centered on XO-2 from the Tycho (TYC) star catalog, and *V* magnitudes for two closeby stars have been labeled. This is a relatively clean field compared to TrES-3 (shown in Figure 4c). XO-2 is part of a binary system so it has a star of comparable magnitude ~30″ South of XO-2. It is therefore named XO-2S [Burke et al., 2007]. The clean field of XO-2 as well as the bright comparison stars make XO-2 a good candidate for differential photometry with a high signal-to-noise ratio.
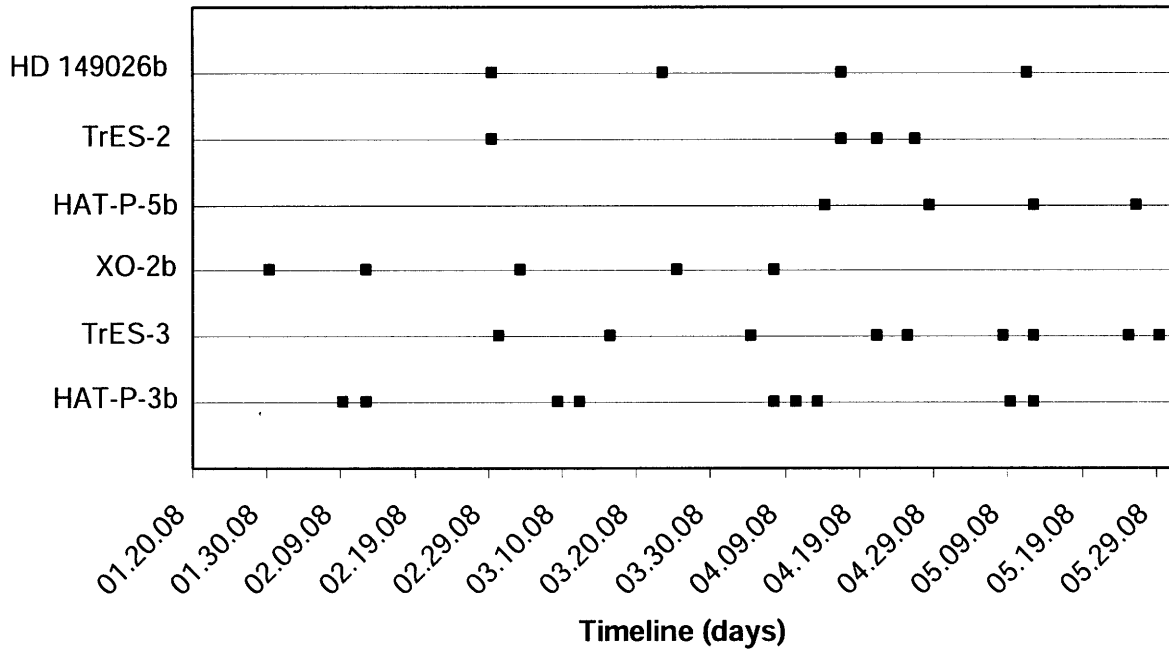
Figure 5. Full transit timeline for high frequency planets for Spring 2008 prediction period. This plot was made using Microsoft Excel. Each square stands for a full transit occurring on a particular day for a particular planet. The transit times used are also in Figure 1. These transit times were deduced by the prediction code described in Section 3.1. HAT-P-3b and TrES-2 are good candidates for building composite lightcurves since they have two or more nearly consecutive full transits.

51
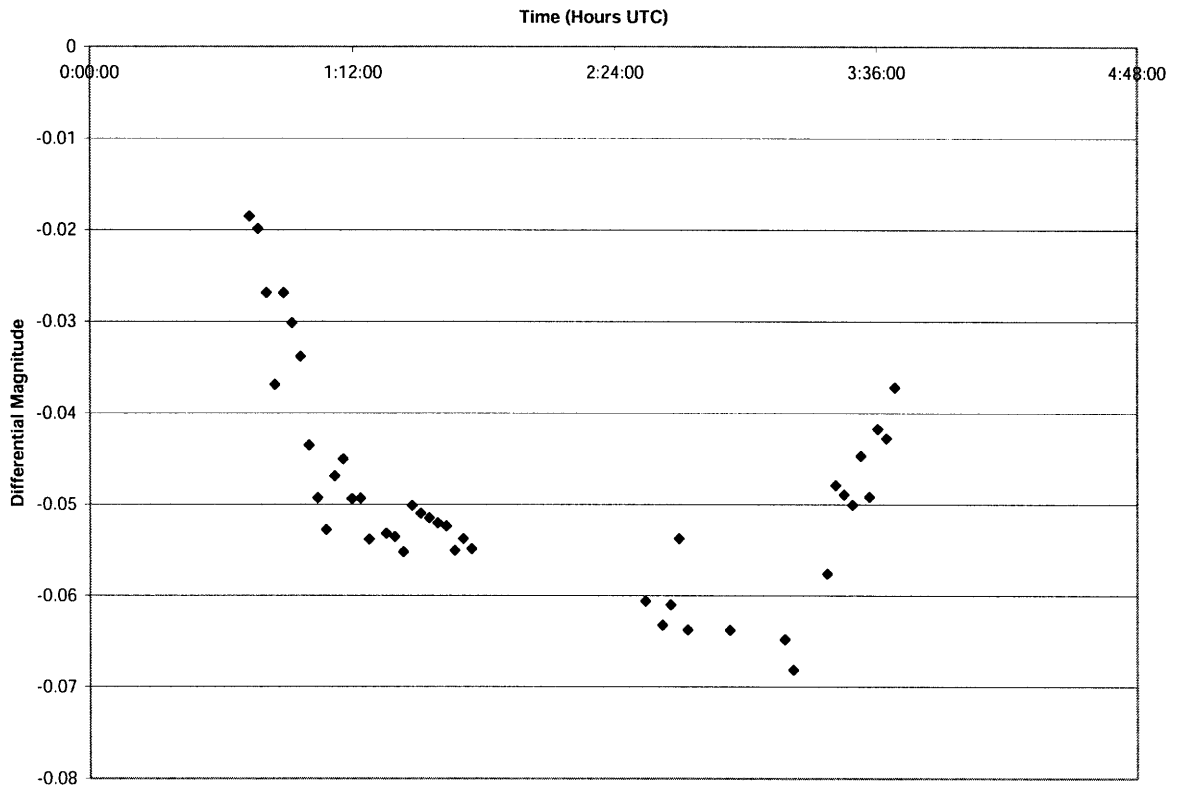
Figure 6. XO-2b transit lightcurve on 03-25-2008 at WAO. The observational data for this transit were taken by Matthew Lockhart, currently a graduate student in PAL on 03-25-2008 from 00:43:40 to 03:43:20 UTC using the 24-inch telescope with the red filter on the POETS CCD. The individual exposure time is 140s. 75 red filter frames were taken resulting in four FITS data cubes. 19 of the 75 red filter frames were unusable due to a severe shift of the telescope such that the target was nearly off of the frame. This results in a gap in the lightcurve around stage 3. 15 dark and 15 bias calibration frames were taken at the end of the night. Differential photometry was performed with XO-2 and comparison star XO-2S (c.f. Figure 4d), with a recorded airmass range of 1.01 to 1.15. The data were calibrated and reduced with "Make_Lightcurve.nb" in *Mathematica 6.0* and plotted in Microsoft Excel. The differential magnitude is plotted against hours in UTC. This lightcurve clearly shows stages 2 and 4 of the transit, with part of stage 3 (c.f. Figure 1). Data for stages 1 and 5 were not taken.

Appendix 2   Tables

TABLE 1.
36 TRANSITING PLANETS AND THEIR PARENT STARS' CELESTIAL COORDINATES.

Planet	Parent star α (hh mm ss)	Parent star δ (° ′ ″)[†]
OGLE-TR-211 b	10 40 15	-62 27 20
OGLE-TR-132 b	10 50 34	-61 57 25
OGLE-TR-113 b	10 52 24	-61 26 48
OGLE-TR-111 b	10 53 1	-61 24 20
OGLE-TR-182 b	11 09 19	-61 05 43
Lupus-TR-3 b	15 30 19	-42 58 46
WASP-4 b	23 34 15	-42 03 41
WASP-5 b	23 57 24	-41 16 38
OGLE-TR-10 b	17 51 28	-29 52 34
OGLE-TR-56 b	17 56 35	-29 32 21
SWEEPS-11	17 59 03	-29 11 54
SWEEPS-04	17 58 54	-29 11 21
CoRoT-Exo-1 b	06 48 19	-03 06 08
CoRoT-Exo-2 b	19 27 07	+01 23 02
WASP-2 b	20 30 54	+06 25 46
HD 209458 b	22 03 10	+18 53 04
HD 189733 b	20 00 43	+22 42 39
GJ 436 b	11 42 11	+26 42 23
XO-1 b	16 02 12	+28 10 11
WASP-1 b	00 20 40	+31 59 24
WASP-3 b	18 34 32	+35 39 42
HAT-P-4 b	15 19 58	+36 13 47
HAT-P-5 b	18 17 37	+36 27 17
TrES-1	19 04 09	+36 37 57
TrES-4	17 53 13	+37 12 42
TrES-3	17 52 07	+37 32 46
HD 149026 b	16 30 29	+38 20 50
HAT-P-1 b	22 57 47	+38 40 30
HAT-P-2 b	16 20 36	+41 02 53
HAT-P-6 b	23 39 06	+42 27 58
HAT-P-7 b	19 28 59	+47 58 10
HAT-P-3 b	13 44 23	+48 01 43
TrES-2	19 07 14	+49 18 59
XO-2 b	07 48 07	+50 13 33
XO-3 b	04 21 53	+57 49 01
HD 17156 b	02 49 44	+71 45 12

[†] This table is arranged in ascending declination, from the Southern to the Northern celestial hemisphere.

TABLE 2.

NORTHERN HEMISPHERE FULL TRANSITS AT WAO FROM 01-20 TO 05-30-2008 BY DATE.

Planet	Date (YYYY M DD)				Time (UTC)	
XO-3b	2008	1	29	1	13	3.752
XO-2b	2008	1	30	3	37	5.7756
HAT-P-3b	2008	2	09	7	51	17.5526
HAT-P-3b	2008	2	12	5	26	42.7996
XO-2b	2008	2	12	5	31	51.9636
HAT-P-4b	2008	2	21	8	17	21.6636
HD149026b	2008	2	29	7	22	3.2913
TrES-2	2008	2	29	9	10	26.5015
TrES-3	2008	3	01	7	50	6.1277
XO-2b	2008	3	04	3	48	7.7988
HAT-P-3b	2008	3	09	7	46	0.4193
HAT-P-3b	2008	3	12	5	21	32.6706
HAT-P-3b	2008	3	15	2	57	5.6759
TrES-3	2008	3	18	7	20	48.4647
HD149026b	2008	3	23	7	30	46.0225
XO-2b	2008	3	25	2	04	56.861
TrES-3	2008	4	04	6	51	31.2317
XO-2b	2008	4	07	4	00	36.0886
HAT-P-4b	2008	4	07	4	36	4.0571
HAT-P-3b	2008	4	07	7	41	56.5236
HAT-P-3b	2008	4	10	5	17	36.1404
HAT-P-4b	2008	4	10	5	57	24.7448
WASP-3b	2008	4	10	6	35	53.9647
HAT-P-2b	2008	4	11	6	12	10.2738
HAT-P-3b	2008	4	13	2	53	16.4415
HAT-P-5b	2008	4	14	7	37	29.9636
TrES-2	2008	4	16	7	45	3.1415
XO-1b	2008	4	17	6	21	35.7776
HD149026b	2008	4	18	4	41	4.2368
XO-1b	2008	4	21	4	58	42.393
TrES-2	2008	4	21	6	20	14.1756
TrES-3	2008	4	21	6	22	20.3143
XO-1b	2008	4	25	3	35	50.453
TrES-3	2008	4	25	4	24	51.5721
TrES-2	2008	4	26	4	55	25.1402
TrES-4	2008	4	26	5	51	28.0668
HAT-P-2b	2008	4	28	3	48	6.0527
HAT-P-5b	2008	4	28	6	13	43.5166
TrES-1	2008	5	03	5	30	32.1617

Planet	Date (YYYY M DD)			Time (UTC)		
WASP-3b	2008	5	04	6	46	57.2756
TrES-1	2008	5	06	6	13	37.8087
TrES-3	2008	5	08	5	53	20.9175
HAT-P-3b	2008	5	09	5	14	46.6859
TrES-1	2008	5	09	6	56	43.7023
HD149026b	2008	5	11	4	50	50.9255
HAT-P-3b	2008	5	12	2	50	32.6883
TrES-3	2008	5	12	3	55	55.4697
HAT-P-5b	2008	5	12	4	50	4.3378
WASP-3b	2008	5	17	5	02	16.3767
HD189733b	2008	5	21	6	47	57.7429
TrES-3	2008	5	25	5	24	37.2187
HAT-P-5b	2008	5	26	3	26	35.0302
TrES-4	2008	5	28	5	29	17.8209
TrES-3	2008	5	29	3	27	15.8324
HAT-P-4b	2008	5	29	3	40	47.3919

TABLE 3.
TRANSIT PREDICTION STATISTICS AT WAO FOR 2007-2009.

Prediction[†] Period	Fall & early winter 2007	Late winter & spring 2008	Summer 2008	Fall & early winter 2008	Late winter & spring 2009
# of total transits	285	334	265	366	357
# of full transits	38	55	45	51	41
# of partial transits	316	279	220	315	293
# of usable partial transits[‡]	69	61	61	59	67
# of unusable partial transits	247	218	159	256	226
% usable transits (full and partial)*	37.54%	34.73%	40.00%	30.05%	30.25%
Highest frequency transiting planets**	XO-3b (12), XO-2b (8), WASP-1b (8), HAT-P-1b (6), HAT-P-6b (6)	HAT-P-3b (11), TrES-3 (9), XO-2b (5)	TrES-3 (12), TrES-2 (8), HAT-P-7b (8), WASP-3b (7) HD189733b (7)	XO-3b (11), HAT-P-6b (6), WASP-1b (8)	GJ436b (10), HAT-P-3b (10), TrES-3 (8), XO-2b (8)

[†] "Fall & early winter" period runs from 09/02-01/11 (132 days including endpoints). "Late winter & spring" period runs from 01/20-05/30 (132 days in 2008, 131 days in 2009). "Summer" period runs from 06/01-09/01 (93 days). Dates chosen according to school term time.
[‡] Usable transits mean all requirements (airmass, Sun, moon separation) fulfilled for >70% of the transit.
* Number of full and usable partial transits over total number of transits.
** Based on planets with the most full or nearly full (>90% of all requirements fulfilled) transits during that prediction period.

TABLE 4.

TRANSIT DURATION FOR HIGH-FREQUENCY FULL TRANSITING PLANETS AT WAO FOR 01/20 TO 05/30/2008.

Planet	Number of full transits[†]	Transit duration (hrs)[‡]
HAT-P-3b	10	2.2
TrES-3	9	1.4
XO-2b	5	2.6
HAT-P-5b	4	2.9
TrES-2	4	1.7
HD 149026b	4	3.2
HAT-P-4b	3	4.2
WASP-3b	3	2.7
XO-1b	3	3.0
TrES-1	3	2.4

[†] This number is calculated based on prediction code described in Section 3.1
[‡] This number is calculated by planet database code described in Section 2.3.

TABLE 5.

OBSERVATIONAL PARAMETERS FOR HIGH FREQUENCY TRANSITING PLANETS, PARENT STARS, AND THEIR NEARBY COMPARISON STARS FOR SPRING 2008 IN DESCENDING FULL TRANSIT FREQUENCY.

Planet	α (hh mm ss) δ (° ' ")	V	I[a]	Relevant Comparison Stars within 30"	Mag.	Transit depth[b]
HAT-P-3b[c]	13 44 22.58 48 01 43.2	11.56	10.52	2MASS 13442345+4801387	$I \sim 15$	~0.97%
TrES-3[d]	17 52 07.03 37 32 46.1	12.40	11.60	Many within 30" of comparable magnitude	various	2.5%
XO-2b[e]	07 48 06.47 50 13 33.0	11.18	10.32	XO-2S	V=11.13	1.5%
HAT-P-5b	18 17 37.50 36 37 16.9	12.00[f]	11.30[f]	TYC2 927 TYC 1090[g]	V=11.2 V=11.4	1.2%
TrES-2[h]	19 07 14.00 49 18 59.0	11.41		No reported bright companions within 30"	N/A	1.4%
HD 149026b[i]	16 30 29.6 38 20 50	8.15		GSC2.3 N63C000350 GSC2.3 N63C000330	V=12.65 V=13.00	0.3%

[a] Blank fields indicate no reported or published value.
[b] All transit depths alculated using R_P and R_* from online Extrasolar Planets Encyclopaedia and Equation 1.
[c] Torres G & Bakos GÁ et al. (2008).
[d] O'Donovan FT, Charbonneau D & Bakos GA et al. (2007).
[e] Burke et al. (2007).
[f] Bakos et al. (2007).
[g] Vizier Online catalog.
[h] O'Donovan FT, Charbonneau D & Mandushev G et al. (2007).
[i] Charbonneau et al. (2006).

TABLE 6.

SAMPLE OBSERVING PLAN FOR TrES-3 TRANSIT PHOTOMETRY FOR A TELESCOPE WITH EFFICIENT TRACKING AND FRAME-TRANSFER CAPABILITY.

	Stage 1	Stage 2	Stage 3	Stage 4	Stage 5
Duration (min)	60	26	26	26	60
Exposure frequency (# of frames per duration)	15 (1 exposure every 5 minutes)	26 (1 exposure every minute)	26 (1 exposure every minute)	26 (1 exposure every minute)	15 (1 exposure every 5 minutes)

TABLE 7.

SAMPLE OBSERVING PLAN FOR TrES-3 TRANSIT PHOTOMETRY FOR A TELESCOPE WITH NO AUTOMATED TRACKING AND NON-NEGLIGIBLE READOUT TIME.

	Stage 1	Stage 2	Stage 3	Stage 4	Stage 5
Duration (min)	60	26	26	26	60
Exposure length (sec)	60	60	60	60	60
Readout time (sec)	~60	~60	~60	~60	~60
# times to adjust telescope[†]	6	2	2	2	6
Total available exposure time (min)	57	25	25	25	57
Maximum exposure frequency (# frames)	**28** (~1 exposure every 2 minutes)	**12** (~1 exposure every 2 minutes)	**12** (~1 exposure every 2 minutes)	**12** (~1 exposure 2 every minutes)	**28** (~1 exposure every 2 minutes)

[†] Assume that it takes a maximum of 30 seconds to adjust the telescope.

TABLE 8.

FULL TRANSITS AT WAO FROM 03-25-2008 TO 04-25-2008, OBSERVING CONDITIONS AND THEIR OUTCOMES.

Date (M-DD)		Planet	Airmass Range[†]	Max. Solar Angle[†]	% Moon Illum.[†]	Min moon distance (°)[†]	Outcome
3	25	XO-2b	1.01-1.33	-9.31	90.3	119	Observed
4	04	TrES-3	1.03-1.58	-19.6	5.21	86.8	74% humidity, rain, fog
4	07	XO-2b	1.09-2.38	-25.4	1.94	80.6	Light rain, haze.
4	07	HAT-P-4b	1.01-2.08	-23.8	2.13	180	Light rain, haze.
4	07	HAT-P-3b	1.01-1.42	*-5.62*[‡]	2.44	150	Close to sunrise
4	10	HAT-P-3b	1.00-1.09	-27.7	23.4	104	Light rain, haze
4	10	HAT-P-4b	1.01-1.39	*2.73*[‡]	57.4	93.2	Close to sunrise
4	10	WASP-3b	1.04-2.31	-14.3	24.0	171	Light rain, haze
4	11	HAT-P-2b	1.00-1.64	-7.57	34.8	125	Went, no data obtained.
4	13	HAT-P-3b	1.00-1.38	-15.7	54.9	73.5	No observer
4	14	HAT-P-5b	1.01-1.52	*-1.11*[‡]	67.6	123	No observer
4	16	TrES-2	1.01-1.38	*-5.02*[‡]	84.9	119	Telescope occupied by another observer
4	17	XO-1b	1.03-1.32	-12.8	91.1	71.4	No observer
4	18	HD149026b	1.00-1.94	-25.4	95.6	75.5	No observer
4	21	XO-1b	1.03-1.67	-23.8	99.4	53.4	Moon too bright and too close
4	21	TrES-2	1.06-1.68	-17.4	99.3	96.4	Light rain
4	21	TrES-3	1.01-1.39	-18.6	99.3	76.2	Light rain
4	25	XO-1b	1.04-2.39	-15.7	81.8	60.9	Overlapped with observed TrES-3 transit
4	25	TrES-3	1.12-2.11	-28.1	81.3	65.2	Observed. Bad seeing.

[†] These data were obtained from the prediction code described in Section 3.1.

[‡] These italicized values indicate a solar elevation angle greater than the -8° limit. These transits were still included in the final list because the Sun only surpassed this limit for less than 30 minutes of Stage 5.